LA--10322-SR

DE85 008903

Accelerator Technology Program

October 1983—March 1984

Compiled by
R. A. Jameson

Los Alamos Los Alamos National Laboratory
Los Alamos, New Mexico 87545

CONTENTS

ACCELERATOR TECHNOLOGY PROGRAM
October 1983--March 1984

Compiled by
R. A. Jameson

ABSTRACT

This report covers major projects in the Accelerator Technology (AT) Division of the Los Alamos National Laboratory. The first sections highlight activities related to beam dynamics, inertial fusion, structure development, the racetrack microtron, and the CERN high-energy physics experiment NA-12.

Discussed next is the the Fusion Materials Irradiation Test Facility, followed by a summary of progress on the Proton Storage Ring and activities of the Theory and Simulation Group. The report concludes with a discussion of the H^- accelerator program and a listing of papers published by AT-Division personnel during this reporting period.

BEAM DYNAMICS

MAGNETIC INSULATION FOR RFQ LINACS

We have investigated the idea that breakdown mechanisms, which require electrons to be transported across the gap, can be inhibited by applying a transverse magnetic field of sufficient strength.[1] In reviewing the currently accepted breakdown mechanisms for the dc case, we have concluded that the most likely rf breakdown mechanisms probably involve both electrons and ions, but need not require that electrons be transported across the gap. Therefore, a transverse magnetic field may or may not play a useful inhibiting role.

Although the gains to be made for the rf case ultimately must be determined by an rf experiment, we have found that a dc experiment reported in the literature[2] demonstrates that (for small gaps) a transverse magnetic field can increase the breakdown field in a way that is qualitatively similar to what would be expected if electron transport across the gap were an important part of the breakdown mechanism. When we apply these dc results to the radio-frequency quadrupole (RFQ), we are able to predict how much electric-field gain is possible for a given magnetic field, and we see the possibility for significant gains in electric field for high-frequency RFQs. These gains translate into an increased current limit for high-frequency RFQs.

We conclude that an rf breakdown experiment should be performed on copper electrodes in a magnetic field. Such an experiment would be important because we do not know how representative the dc results are for the rf application. We have also concluded that a magnetic field parallel to the RFQ axis is the most attractive configuration.

REFERENCES

1. T. P. Wangler, "Magnetic Insulation For RFQ Linacs - An Idea With Significant Potential Gains," Los Alamos National Laboratory memorandum AT-1:83-336, November 8, 1983.

2. V. A. Petrosov and N. V. Cherkasskii, "Effect of a Transverse Magnetic Field on the Breakdown in a High-Vacuum Discharge Gap," Sov. Phys.-Tech. Phys. 22, 565 (1977).

ACCELERATOR INERTIAL FUSION

DESIGN CONSTRAINTS FOR A RADIO-FREQUENCY-LINAC/STORAGE-RING DRIVER

Since work on heavy-ion fusion began in the middle 1970s, a number of specific rf-linac/storage-ring accelerator designs have been presented in various reports. In most cases, less emphasis has been given to presenting methods for generating designs that satisfy the most important physics constraints. We have reviewed the equations that must be satisfied when generating rf-linac/storage-ring systems for heavy-ion fusion, including current amplification and space-charge limits. To treat the phase-space constraints, we have derived new formulas for separate transverse and longitudinal available dilution factors in terms of parameters of the rf-linac/storage-ring system. These formulas allow a more complete specification of the phase-space constraints. We used the results of a published systematic target study and expressed the results in a form that allows a more convenient selection of parameters at fixed target gain. We outlined a method for generating accelerator designs that satisfy the target, current amplification, phase-space, and space-charge constraints—and as an example, we applied this method to generate and compare designs for ^{208}Pb with charge state q = +1.

We conclude that, in principle, the phase-space constraints can always be met by proper design to provide adequate available dilution factors. The dilution factors can be increased at the expense of reduced target gain; at fixed gain, they can be increased within certain limits, either at the expense of additional components or at the expense of larger total beam energy E. The penalty in both cases probably is cost.

REFERENCE

1. T. P. Wangler, "Some Design Constraints For An RF-Linac/Storage-Ring Driver," submitted to INS International Study on Heavy Ion Accelerators and Their Applications to Inertial Fusion, January 23-27, 1984, University of Tokyo, Japan, Los Alamos National Laboratory document LA-UR-84-177.

ACCELERATOR STRUCTURE DEVELOPMENT

RFQ ANALYSIS

Work has begun on a multiport network solver (MPNS) that will have the capability of determining stored-energy distributions and tuning-error sensitivities for complex networks of transmission lines and lumped-circuit elements. This program will be very useful for studying the properties of resonantly coupled manifold-RFQ systems as well as for determining the effectiveness of RFQ shorting rings versus structure parameters. By the end of March, the data-manipulation algorithm was completed, and much progress was made on understanding the mathematical details of embedding arbitrary combinations of lumped and distributed circuits in 2N-port networks. The problem of calculating the properties of embedded systems has been solved.

RFQ SHORTING RINGS

Experience with tuning an RFQ with (nearly) periodic shorting rings has improved our qualitative understanding of the effects and side effects of shorting rings. Figure 1 shows the dipole modes of the RFQ pushed up by shorting rings with nonzero inductance. This can be compared to Fig. 2, which shows the modes for an RFQ with no shorting rings.

The ease with which tuning errors mix dipole modes into the field distribution depends inversely on the mode spacing. If the shorting rings have sufficiently low inductance, the dipole modes can be raised high enough in frequency to significantly reduce the effect of tuning errors on the dipole mixing. Thus, the symmetry of the azimuthal field will be preserved.

The rings have a side effect that makes it unprofitable to arbitrarily add many rings to the RFQ. These rings add a periodic capacitive loading to the RFQ quadrupole mode that results in a distortion of the mode spectrum and the longitudinal field distribution.

Figures 3a-3d show the effect of various tuning conditions on the longitudinal field distribution and show the "clothespinning" effect that occurs because of the capacitive loading. The field level is reduced quadratically away from the shorting rings.

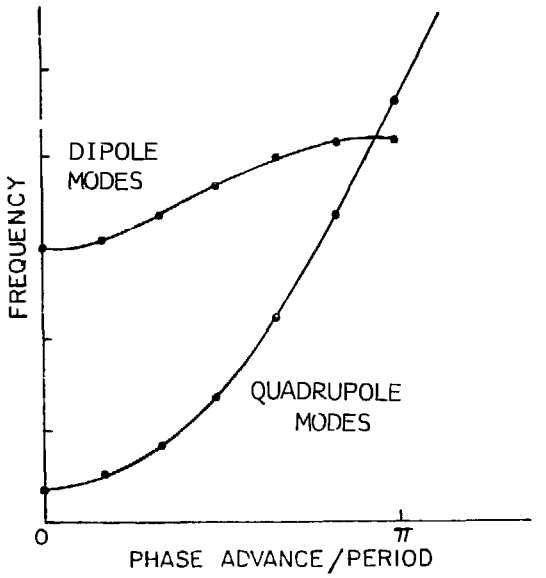

Fig. 1.
Mode spectrum for RFQ with shorting rings. The upper curve shows the dipole-mode passband; the lower curve shows the quadrupole mode passband.

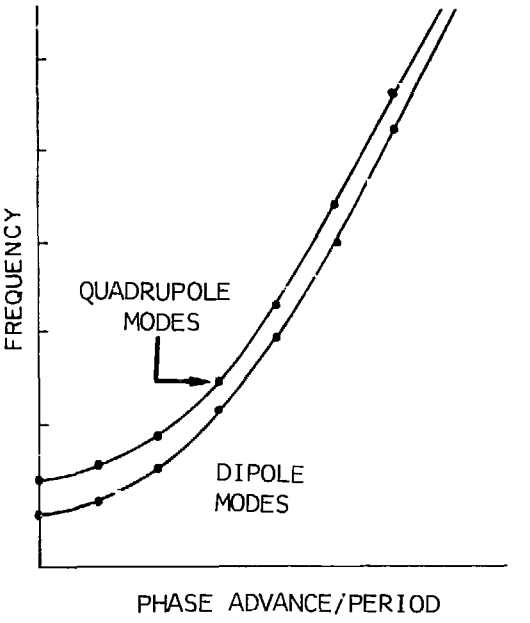

Fig. 2.
Mode spectrum for RFQ with no shorting rings. The upper curve shows the quadrupole passband; the lower curve shows the dipole passband.

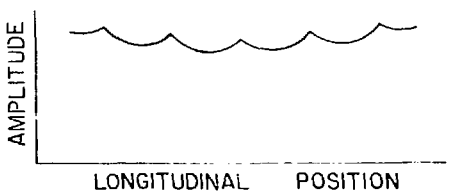

Fig. 3a.
Field amplitude versus longitudinal position for frequency above unloaded cutoff frequency.

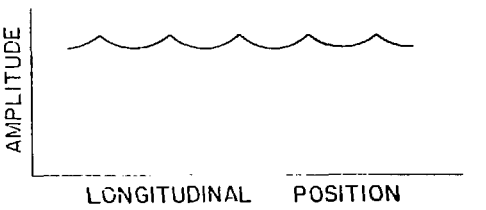

Fig. 3b.
Field amplitude versus longitudinal position for frequency slightly above loaded cutoff frequency.

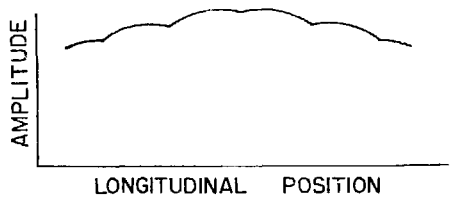

Fig. 3c.
Field amplitude versus longitudinal position for frequency below loaded cutoff frequency.

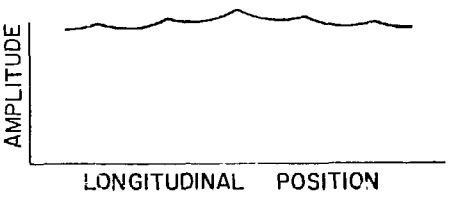

Fig. 3d.
Field amplitude versus longitudinal position at cutoff frequency of loaded system.

LUMPED-CIRCUIT MODEL OF THE FOUR-VANE RFQ RESONATOR

We make use of the result that large capacitive vane loading in the four-vane RFQ resonator allows a convenient representation of this resonator by a simple lumped-circuit model.[1] Formulas are derived for magnetic field B, power per unit length P_ℓ, stored energy per unit length W_ℓ, and quality factor Q, which depend on frequency, intervane voltage, and a single unknown parameter, the vane capacitance per unit length C_ℓ. The computer program SUPERFISH was used to calculate the electromagnetic properties of the RFQ cavity. These calculations were used to determine C_ℓ versus the dimensionless parameter r_o/λ, where r_o is the radial aperture and λ is the free-space wavelength. For the cases studied, we have found that the P_ℓ values agree to better than 10%; whereas, the B, W_ℓ, and Q values agree to better than 5%.

The model can be useful for estimating cavity properties in the early stages of an RFQ design and for showing the dependence of the cavity properties on ω, C_ℓ, and V.

REFERENCE

1. T. P. Wangler, "Lumped-Circuit Model of 4-Vane RFQ Resonator," Los Alamos National Laboratory memorandum AT-1:83-348, November 15, 1983.

RACETRACK MICROTRON

ACCELERATING SYSTEM

Following a decision in September 1982, to abandon the disk-and-washer rf structure for the racetrack microtron project, a water-cooled side-coupled structure (SCS) was designed and modeled. A 2.7-m SCS was later built as part of the 5-MeV injector. This preaccelerator section was designed to accelerate the electron beam from 1.3 to 5 MeV with an accelerating gradient of 1.5 MeV/m. Fabrication of this section was completed in February 1983 and was tested at cw power levels that exceeded the design operating level by 60%. The SCS has proved to be highly successful in all respects. It exceeds its design specifications on shunt impedance (82.5 MΩ/m observed versus 80 MΩ/m goal), voltage gradient (2.0 MV/m observed versus 1.5 MV/m goal), and power-dissipation capability (49 kW/m observed versus 28 kW/m goal). Following the successful test of the preaccelerator, we proceeded with the fabrication of the remaining rf structures.

The capture section was completed in FY 84. This section was designed to accelerate the electron beam from 100 keV to 1.3 MeV. The structure, 0.8 m long, consists of 14 individual side-coupled cells whose lengths are programmed for electron velocities increasing from 0.55 to 0.97 times the speed of light. The capture section was operated at power levels 20% in excess of the design operating point.

Fabrication of the main accelerator sections is well under way. This pair of 4-m-long tanks is designed to accelerate the relativistic electron beam 12 MeV per pass. The first 2 m of this accelerator is now complete.

CHOPPER/BUNCHER SYSTEM

Before injection into the capture section, the electron beam will be both chopped and bunched into 10° bunches containing one-sixth the total gun current. To accomplish the chopping, the 100-keV beam passes through a deflection cavity excited in two equal-amplitude, orthogonal transverse modes with a 90° phase shift between them. The cavity fields deflect the beam in a conical figure, forming a circle on an aperture plate. The aperture in the plate is sized to pass a total of 60° of the arc, or one-sixth the cw beam. A split solenoid lens then images the "chopped" beam emerging from the aperture at the second

chopping cavity. The transverse modes in the second cavity are adjusted so that the transverse momentum imparted to the beam by the first cavity is exactly cancelled.

The beam then passes through a buncher cavity where longitudinal fields compress the 60° beam spread into ±5° at the entrance to the accelerator. All of this beam later will be captured and accelerated by the capture section.

The design for this entire system was completed and modeled in FY 84, and fabrication of components was begun. The complete chopper/buncher system (including three beamline rf cavities, five rf power amplifiers and their associated fast-phase and analog control loops, plus a computer control system) has since been completed and tested. This turnkey system was accepted and delivered to the NBS in the spring of FY 84.

RADIO-FREQUENCY POWER SYSTEM

The 500-kW main rf power stand for the microtron was completed in FY 83 and was used in power tests of the capture section. Earlier tests were precluded by an ∿10% ripple at full power, which originated in a 65-kV, 16.5-A klystron power supply. The problem was diagnosed as an imbalance of the three-phase line caused by the variable transformer. The vendor has since built and installed new sets of compensation coils at both Los Alamos and the National Bureau of Standards (NBS). The Los Alamos power supply now meets its 1% ripple specification; unfortunately, the vendor's modification to reduce the ripple also reduced the input impedance by a factor of 2. The resulting surge currents during turn-on and crowbar exceeded the stress rating of some components, and the supply has now failed. The NBS supply presumably has the same weakness. It will be first tested under load when the accelerator structures are delivered in the summer of FY 84.

A new, space-saving, spark-gap crowbar was designed and built in FY 83. During power tests of the capture section, the spark gaps themselves were found to be unreliable. This design has now been abandoned and a compact, but conventional, ignition crowbar is now under construction.

CONTROL SYSTEM

This reporting period resulted in continued development of the distributed intelligence approach. The rf secondary station was used to control the

chopper/buncher system, and the primary station was further developed to provide more convenient operator interface with the system devices.

At the secondary station level, the old control panel was redesigned to permit multiple interrupts, thus allowing for better operator response. Hardware and software changes were made to improve remote operation. As preparations were made to deliver the chopper/buncher system to NBS, final testing and preparations were made to the rf secondary control station's physical rack and documentation. The magnet power supplies, which form a major tertiary station subsystem, were cabled.

In the primary station, software and hardware improvements were made in the link system to improve the reliability. The high-resolution color terminal was also received and checked out for the primary station. Much software remains to be written to support this unit. Several operator-convenience features were added to the primary-station software per requests from NBS. An applications program subsystem was installed, and progress was made toward its complete implementation. The system is now working in the primary station. No applications programs have yet been written that use the system, however.

STRUCTURE STUDIES

We have studied the effect of cutting-tool type and cutting speed on the Q of seven test accelerating cavities at 2380 MHz. Carbide, polycrystal diamond, and single-crystal diamond tools were used in this test. With each tool, a cavity was finish machined on a lathe at 625 and 2000 rpm. An additional cavity was machined with the single-crystal diamond at 1125 rpm. A sulfur-free cutting fluid was used in all cases.

The Q was measured on the seven cavities by fastening each cavity in a clamping fixture. All measured Qs were within 95% (±1%) of the value predicted by SUPERFISH. The cavities then were brazed in a hydrogen brazing furnace at 1550°F with CuSil. The resulting measured Q values were all within 98.7% (±0.4%) of SUPERFISH value.

A conclusion reached after these tests was that no improvement in Q can be obtained by using diamond tooling instead of carbide. However, the diamond did give a smoother finish as observed under a microscope.

After completing the individual cavity tests, two seven-cell accelerating structures were built to compare the effective shunt impedance of the coaxial structure and the SCS at 2450 MHz. The coaxial structure was designed by the

University of Illinois, and the side-coupled model was designed by Los Alamos. The resulting measurements are summarized in Table I. The measurements of ZT^2/Q will be further refined, but the Q measurements are believed to be accurate to within 0.5%.

TABLE I

MEASURED RESULTS FROM COAXIAL AND SIDE-COUPLED MODELS

	Coaxial Model	Side-Coupled Model
Q	16410	16400
Q percentage of SUPERFISH value	91	91
ZT^2/Q	5393	5650
Per cent of theoretical ZT^2/Q	103	102
Coupling per cent	3.4	2.7
ZT^2 (MΩ/m)	88.5	92.7

CERN EXPERIMENT NA-12

This collaboration, NA-12, at the CERN Super Proton Synchrotron (SPS) with groups from France, Belgium, and the USSR was initiated in 1981 for an experimental study of π-$\bar{p}$ interactions at 300 GeV/c. The initial contribution of the Los Alamos group was to provide fast-analog-trigger circuitry for the experimental apparatus that allows an entirely new area of physics to be investigated with the existing GAMS photon detector. This system is just now being put to use, and preliminary results are encouraging.

The fast-trigger circuits have been installed in one-quarter of the GAMS detector. Cabling from the GAMS detector to the counting house for all the fast-trigger circuits was also installed. Tests have been made regarding the effect of the circuits on the existing data-acquisition hardware of the GAMS detector. No visible effect has been observed. Progress has been delayed on installation of the circuits in the remaining three-quarters of the detector because of problems with the detector.

The modular electronics that fan out the fast-trigger signals has been installed in the counting house and has been tested for linearity, noise levels, and gain variations between channels. We found that channel-to-channel gain variations were, in most cases, less than 1%. No channel had a gain that varied more than 5% from the mean. Discovered in the system were minor problems concerning the linearity for signal levels that were somewhat smaller than nominal. For these problems, corrections that involve minor alterations to the circuits are in progress.

During the data-taking run in September 1983, some preliminary data were taken with the Los Alamos trigger system. The principal aim of the exercise was to get some idea of the rates to be expected when triggering for the production of 3- to 4-GeV/c particles that decay into two photons. The rates were small enough that the data-acquisition system was not swamped with events. The trigger rate for an incident pion beam of 1×10^7 particles/s is estimated to be between 10 and 100 events/s.

A total-absorption cellular hadron calorimeter recently has been added to the experimental setup. This calorimeter is placed directly downstream of the GAMS detector and covers a slightly larger area. The calorimeter consists of a central section, which is a 10 by 10 matrix of 10- by 10-cm counters. The central section is surrounded by four layers of 20- by 20-cm counters. Each

cell is a sandwich of thirty-five 2.5-cm iron converter plates interleaved with thirty-five 0.5-cm-thick sampling scintillators. This sandwich represents ∿50 radiation lengths and ∿16 nuclear-absorption lengths of material. The light from each cell is collected through wavelength shifter bars and is monitored by a photomultiplier tube and electronics identical to that used in the GAMS detector. The 240 calorimeter cells were calibrated and the entire unit was assembled.

A prototype of the calorimeter gave a spatial resolution of 0.7 cm for the 10-cm cells and 1.5 cm for the 20-cm cells with 200-GeV/c hadrons. Energy resolution of the calorimeter corresponds to a resolution of ∿4.6% for 200-GeV/c hadrons.

Most neutral kaons escape detection in the guard system, but they are detected in the GAMS detector, appearing to be low-energy photons. All K_L^0 mesons will be detected in the hadron calorimeter. The pions from K_S^0 mesons decaying into two neutral pions also will be detected in the GAMS detector. The pions from K_S^0 decaying into two charged pions will be detected by the hadron calorimeter while simultaneously being measured by proportional chambers placed upstream of the calorimeter. Identification of these components as hadrons and the measurement of their position and energy by the hadron calorimeter improve the background rejection for rare multiphoton events and allow the full exploitation of the exclusive neutral trigger, including those processes that contain neutral kaons. The calorimeter will also be useful in conjunction with inclusively triggered events. The analysis of the first usable data, taken during the summer of 1982, is now in progress.

FUSION MATERIALS IRRADIATION TEST FACILITY

International funding by the member nations of the International Energy Agency is still being negotiated. The present expectations are that the agreements will support an FY 86 restart of final design and construction activities for the Fusion Materials Irradiation (FMIT) Facility. In the interim, the development of the accelerator, lithium target, and support facilities is being continued as funding permits.

We were forced to conclude the initial operation of the 2-MeV accelerator because of an rf-induced failure of one of the O-rings on the vacuum end closure of the RFQ manifold. Before the vacuum failure occurred, we were able to operate cw at power levels of 160 kW for short periods (the design power level is 350 kW). Outgassing continued to be the major limiting factor in attempts to operate at higher power levels. External-temperature maps indicated the possibility of some thermal anomalies in the RFQ, associated with cooling-water access boxes between the core and manifold tanks. Because the RFQ had to be removed from the beamline to repair the vacuum seal, the structure was disassembled, and the source of both the outgassing and thermal difficulties was revealed. Therefore, most of this reporting period was devoted to the design and implementation of those changes required to eliminate all the anomalous effects observed during initial operation. In spite of the difficulties, we were satisfied that the basic design and engineering of the RFQ was sound; only a modest redesign of a few components was necessary to correct all the problems.

ACCELERATOR

Operation

The 2-MeV accelerator program was suspended in October 1983 because of the failure of a vacuum O-ring seal. At that time, rf conditioning of the RFQ was taking place with the goal of achieving cw operation at the design power level. Repair of the vacuum seal required disassembly of the RFQ; therefore, an extensive study was begun, not only to solve the overheating problems but also to improve the mechanical assembly. Improvement of the vane-adjusting mechanism allowed the RFQ to be adequately tuned by simple vane movement, hence eliminating the troublesome tuning straps on the vane ends. At the same time, the

profile of the boxes covering the vane cooling lines was reduced to eliminate the heating problem that led to the failure of the vacuum seal. Finally, the complicated capacitor plate assembly was replaced with a coaxial design, thereby eliminating four gold-wire rf seals and considerably simplifying the assembly procedure.

We had noticed that the resonant frequency of the RFQ sometimes changed by several kilohertz over several milliseconds during pulsed operation. This effect was traced to mechanical vibration of the parallel-plate capacitor ring. The new coaxial capacitor is considerably more rigid than the parallel-plate design and is expected to eliminate the rapid frequency response of the structure.

During the rf conditioning, the primary limitation to increasing the drive power was insufficient vacuum in the RFQ. Residual gas analyzer (RGA) measurements determined the dominant gas component to be molecular hydrogen. The source of this gas load is several RFQ components that were hydrogen-furnace brazed. At low duty factors (typical of most accelerators), the hydrogen absorbed in the metals during the brazing poses no problem because of the low average power dissipated in the structure. We find excessive hydrogen evolution for duty factors greater than 15%.

Another adverse effect of the outgassing was the inability of the ion pumps to pump the large hydrogen-gas load without overheating. We found not only that the heated ion pumps had a greatly reduced pumping speed, but also that, at times, the pumps evolved more gas than they were pumping. Replacement of the ion pumps with cryopumps allowed us to maintain an acceptable vacuum.

To solve the hydrogen outgassing problem, the hydrogen-furnace brazed components were vacuum-furnace baked at 400°C for 24 h to eliminate any remaining hydrogen. In addition, we know that titanium plating of copper surfaces is effective in reducing outgassing rates by a factor of 10 or more. Furthermore, the titanium coating is also beneficial in the reduction of multipactoring; therefore, we developed techniques to coat all internal surfaces of the RFQ with a thin layer of titanium (10 to 20 μm). The standard technique of vapor deposition from a hot wire (followed by venting to dry nitrogen) deposits, primarily, a layer of titanium oxide because the heat formation of titanium nitride is insufficient to break the triple bond of the nitrogen molecules. Hence, the layer is not very durable and wipes off easily. We, therefore, developed a technique to form a titanium nitride layer over the thin metallic

coating. This layer is very durable and resists wiping. The technique involves the evaporation of the titanium with a partial pressure of 1 μm of ammonia gas in the structure.

After the RFQ was reassembled and reinstalled, the loaded Q of the improved structure was 6600, an increase from the previous value of 5500. The higher Q will reduce the rf power losses in the cavity and, simultaneously, will reduce the drive power and cooling requirements. While we were measuring the Q of the RFQ, we found the manifold slug tuners were resonating at frequencies near those of the RFQ operating frequency. By lengthening the straps used to shunt the rf current that normally would be conducted by the stainless steel bellows, we drastically lowered the resonant frequency of the slug tuners—thus solving the problem. Electrical measurements on the individual slug tuners confirmed that the problem was resolved.

The rf operation was resumed on March 27, 1984, and initial indications are very good. The frequency is stable and does not change more than a few kilohertz during rf operations; most of this change is due to fluctuations in the cooling-water temperature. No rapid frequency changes have been observed. Hence, the coaxial capacitor design has eliminated the mechanical vibrations of the old capacitor design. After a few initial excursions into the 10^{-5} range, the vacuum pressure has stabilized in the low 10^{-6} range. The RGA indicates the primary gas component is still molecular hydrogen, but the pressure is much improved over previous operation. At this time we have no indication of the nature of titanium-coating effects on multipactoring. However, if substantial multipactoring were occurring in the RFQ, the voltage standing wave ratio (VSWR) likely would be worse than the presently measured value of 1.10.

Linac

In the past, the fields in a drift-tube linac (DTL) were stabilized with posts one-quarter-wavelength long that were resonantly coupled to the drift tubes. In the FMIT DTL, the ratio of the drift-tube diameter to the tank diameter is so low that the end of a post (one-quarter-wavelength long) is too far from the drift tube for adequate coupling. We have been investigating the feasibility of using the next highest oscillation mode of the post, namely the three-quarter-wavelength (3/4) mode. Because the 3/4 mode has too high a frequency unless the post is excessively long, a relatively short extension of the

post outside the tank is capacitively loaded at a point some distance from its shorted end to lower the resonant frequency of the 3/4 mode.

Seven post couplers are required in the sixteen-cell DTL if every other drift tube couples to a post. In the first attempt to test 3/4 post couplers, we built seven aluminum stubs extending the 1.1-cm-diam posts 6.35 cm beyond the inside wall of the tank. The stub had the geometry of a short piece of coaxial transmission line with a characteristic impedance of 49 Ω. Provision was made to install a variable shunt capacitor about 3.5 cm from the shorted end of the stub. Unfortunately, we were unable to lower the 3/4 frequency to the desired 368-MHz frequency with this arrangement. Calculations for a transmission-line model of these slightly extended and capacitively loaded post couplers suggested that we were unable to tune the 3/4 mode to the desired frequency because the stub was simply too short and would require far more loading capacitance than we could reasonably supply.

We then constructed another set of seven cold-model couplers for the 4.6:1 model. The original posts for this model were not scaled correctly from the DTL prototype. For the new post couplers, the post diameter was scaled from the prototype post couplers and the stub's inside diameter was scaled from the diameter of holes already in the side of the DTL full-sized tank. The characteristic impedance for stubs scaled in this manner is 28 Ω. The stub lengths are continuously variable between 5 and 20 cm, and the loading capacitor may be installed anywhere along the length of the stub.

We succeeded in tuning the 3/4 mode of these post couplers to a wide range of frequencies covering the operating range for various combinations of stub length and loading capacitance. We also identified the band of seven post modes with the seven couplers installed in the DTL model. Now we are working on the next step, namely, to tune all of the posts for resonant coupling to the drift tubes.

Instrumentation and Control System

The beam diagnostics effort has been integrated into the Instrumentation and Controls (I&C) Section. During disassembly of the RFQ, we had time for some additions and improvements to the Facility Control Systems (FCS). Additional temperature channels were added to the RFQ structure as an aid in mapping the temperature distribution. The beam emittance codes, originally written by EG&G, were modified to work within the framework of the FCS; now, an

operator at the control console can obtain emittance plots from real-time data by using the touch panel control. A code to monitor the beam position has been modified to speed up the response of the bull's eye display. As the reticon detectors become available, this code will be fast enough to give real-time response (three to four updates/second).

The I&C effort to support the rf system from the FCS has been completed, and testing will begin as the rf control chassis are completed. The Pearson transformer has been installed and connected to the FCS.

The RGA has been connected to the FCS. A local node display of the RGA output is operational. The data logging system is recording the RGA output onto the disk.

The temporary withdrawal of funds from the EG&G effort resulted in a rescheduling of that effort. The reticon hardware being developed by EG&G should be available in November.

The Local Control Program (LCP) has been updated to support the requirements of each node. The resulting LCP is operational in all nodes, is consistent from node to node, is smaller, and runs faster.

The alarm code resides in the primary control computer and receives data messages from a surveillance code residing in each node. The data messages notify the operator of any alarm condition and prompt him to store the data onto the disk. These codes have been rewritten to add some desirable features. The operator can suspend the surveillance code in any or all nodes, as required. The new version of the code supports changing some parameters in the node databases during accelerator operation. A database editor has been written to interface with the operator and accomplish the required database changes. A user-friendly method of presenting and plotting any recorded accelerator data has been installed and is operational.

The data communications system being used between the FCS computers is the DECNET package supplied by Digital Equipment Corporation (DEC). This package is adequate to use on the 2-MeV prototype but has the disadvantage of using a large amount of computer memory in each computer on the network. An alternate data communications system (ethernet) is reaching maturity; standards have been adopted and several vendors have marketed hardware for it. An investigation of ethernet has been started and preliminary tests show an order-of-magnitude increase in message transfers. Equipment has been ordered to permit a testing of four microcomputers on an ethernet link. Software drivers for message

transfer have been written. If this investigation indicates a significant improvement in message transfer rates and a decrease in the amount of required computer memory, testing of ethernet on the 5-MeV prototype will be proposed. The software structure of the FCS would permit this change rather easily.

An agreement has been reached that Hanford Engineering and Development Laboratory (HEDL) will provide facility wiring documentation for FMIT, using an existing computer program. The facility wiring documentation for the prototype accelerator will be done using the DEC-supplied query language (Datatrieve) that is being used for the data channel main database. The input format has been designed, and the several required output reports have been completed. Accumulation of data for input to the system has been started.

A microcomputer system with supporting software has been assembled to assist in tuning the RFQ, which made the RFQ tuning proceed much faster.

An instrumentation committee has been formed to propose standards for accelerator instrumentation. A charter has been adopted and subcommittees have been appointed to study various aspects of the standardization problem.

Vacuum System

A special high-capacity hydrogen cryopump from Varian Associates, Inc., Palo Alto, California, was evaluated on the low-energy beam transport (LEBT). Pump performance has been excellent, and the capacity exceeds the manufacturer's specification of 39 ℓ/s at STP for hydrogen. This should provide well over 100 h of LEBT beam-on service with the present ion source before regeneration is required.

The problem of high hydrogen pressure in the RFQ has been addressed by switching from ion pumps to cryopumps and by vacuum bakeout of RFQ components that were brazed in a hydrogen furnace. Ion pumps regurgitate hydrogen from their titanium plates as the plates heat. Because heating increases with operational pressure, this hydrogen evolution causes thermal runaway in the low 10^{-5} torr range. There is now only one ion pump on the RFQ, the other two having been replaced by cryopumps.

The rf System

As a result of the damage to the RFQ structure reported above, rf operations were suspended for most of this reporting period while repairs and

modifications were made. During this time, the rf system controls were consolidated, and numerous monitors were added to allow better supervision of operation, ultimately from the computer control center. No changes were made to the rf system itself because operation before shutdown had been entirely adequate in spite of the difficulties with the RFQ.

The question of frequency control, raised during initial operation, cannot be addressed until the thermal behavior of the structure under high power is more fully understood. (This is the main reason for all the additional monitors.) In the meantime, a frequency synthesizer is being used under operator control.

Rapid frequency modulation is no longer required to track cavity frequency because the oscillation mentioned in the previous report has been eliminated by redesign of the manifold tuning capacitors. However, the slug tuner still cannot be used to hold the RFQ on a fixed frequency without disturbing the power balance between core and manifold and at high power, disturbing the temperature distribution in the tank, causing both VSWR and power balance changes.

To study this behavior, rf monitor loops and probes have been added in the RFQ as follows.

- Three loops (located along both sides of the top and bottom vanes, one near each end and one near the center) have been mounted in the vane base near the tank wall. All 12 signals are brought out the upstream end wall through coaxial ceramic bushings, 6 at the top and 6 at the bottom. Solid sheath coaxial cables of equal length connect the loops to two six-position electrically actuated coaxial switches so that any of the signals may be monitored at the rf control rack through two calibrated RG 8/U cables.
- One additional loop in the top-port quadrant is opposite the center-port loop on the top vane. This signal is also brought out the end wall, but is not switched. It is transmitted through foam-flex cable directly to the low-power rf racks and is used as the feedback signal for phase and amplitude control.

- Four E-field probes in the manifold are located midway between the ends, opposite the vane bases (between the slug tuners). These probes are monitored through a third coaxial switch, together with the two manifold loops incorporated originally. (The latter are located on the port side near the tuning capacitors at each end.)
- Two probes are located under the port and starboard vanes where there should be no field. These probes are monitored through a fourth coaxial switch, together with the core end-wall loops used previously.

A control panel has been added to allow selecting any of these signals, either manually or from the computer control center, to measure amplitude and/or phase relative to the feedback signal. Some data have been logged by the control system, but to date they have not been helpful in analyzing the problem. It is expected that when somewhat more stable operation is obtained, systematic data logging and subsequent plotting may help to analyze gradual changes in the field patterns in the tank.

All other controls necessary for operation of the rf system during processing of the RFQ have been consolidated into two chassis, located near the center of the low-power rf complex. One of these, called the Chain Control Panel, allows ON/OFF control and monitoring of the high-power amplifier and other equipment associated with one amplifier chain. The other, called the System Control Panel (SCP), allows adjustment of all phase and amplitude set points, selection of one of two rf amplifier chains for operating either the RFQ or DTL, and selection of manual or computer control. The SCP also indicates the status of system interlocks, such as tank vacuum and water cooling, and resettable fault-protection circuits, VSWR and optical arc detector, on all four chains. Provision is made for resetting the VSWR circuits remotely, either manually or by the computer, and for removing high voltage from all four chains simultaneously. Both panels incorporate "Emergency Off" buttons. Flashing warning lights, signifying high-power rf operation, are controlled through these panels. Also, the Vac-Ion power supply used for tetrode and window pumps is interlocked for safety and protection against loss of tank vacuum.

PROTON STORAGE RING (PSR)

PSR CONSTRUCTION

An important PSR milestone was achieved when building construction was completed in December 1983. The contractor, Davis and Associates of Santa Fe, did an excellent job and actually finished 2 months ahead of schedule. All mechanical equipment associated with the buildings is now operating properly.

Installation of PSR equipment began in January 1984, immediately after building completion.

The 7 dipole magnets and 12 quadrupole magnets needed in the PSR injection and extraction lines have been installed and rough aligned. The magnets are being connected, and the vacuum pipes are being placed. Installation of the equipment in the sloping portions of injection and extraction lines will be completed during the spring 1984 shutdown of LAMPF (before June 15).

Installation of wiring and electronic racks in the PSR equipment building also is proceeding rapidly. The vacuum control racks and 2.8-MHz-buncher power supplies are in place. At the end of the report period, we were slightly ahead of schedule on equipment installation.

Listed below are some other highlights, reflecting the status of PSR equipment procurement and development, and plans for first beam tests.

- A comprehensive tune-up plan has been developed for the long-bunch mode. It calls for reaching 20 μA by October, 1985 (with some beam for users), and 100 μA in the fall of 1986.
- The LAMPF switchyard-kicker prototype has operated at full power, meeting all performance specifications for pulse rise time, flat-top regulation, and repetition rate.
- The 2.8-MHz buncher has operated at up to 15 kV with one-half of the power amplifier. Satisfactory functioning of the common-anode-configured amplifier (with no oscillations) at design power levels has thereby been demonstrated.
- The injection-chopper traveling-wave deflection structures and high-power-pulse amplifiers have been completed.
- All injection- and extraction-line magnets have been received, and check-out has been completed.

- The magnetic field mapper for measuring the ring dipoles has been brought up to a satisfactory operational state and is ready to begin mapping at a precision of one part in 10^4.
- Data acquistion and display programs have been written and demonstrated for the beam-position-monitor (BPM) system and for the run-permit system.

PSR LONG-BUNCH-MODE TUNE-UP PLAN

During this reporting period we have developed, collaboratively with the staff of the Physics and Meson-Physics Divisions, a detailed plan for commissioning the PSR in the long-bunch mode through the end of 1985. Elements of the plan and the schedule for their implementation are shown in Table II. We assume a start on the detailed tuning program by mid-June, and also assume that first beam in PSR will have been achieved in April, with some very preliminary studies carried out at that time (including a first correction of the closed orbit).

As soon as beam is available in 1986, high peak-current tuning will continue. As losses are understood and controlled, average beam current will be gradually increased, with the objective of reaching 100 μA in routine operation by the end of 1986.

We assume that the following equipment will not be available at the beginning of the 1985 tune-up program:

- Line-D bunch rotator
- 503.125-MHz buncher
- Injection-line programmed steerers
- Octupoles and sextupoles
- Fast transverse damper
- Sophisticated stored-beam profile diagnostics

TABLE II

SUMMARY OF LONG-BUNCH MODE TUNE-UP PLAN (1985)

Activity	Time (Months)	Start Date
• Measure LAMPF beam properties • Set injection trajectories and tune-stripping process • Re-establish closed orbit • Learn how to use orbit bumpers	0.50	6/15
• Learn how to use 2.8-MHz buncher • Learn how to use extraction system	1.00	7/1
• Tune extraction line to target	0.25	8/1
• Bunching studies at low beam intensities	0.50	8/8
• Tuning at intermediate current (20 μA)	1.50	8/22
• Beam on target for users (20 μA) • Initial high peak-current tests Scheduled time: 70% - users 30% - machine studies	2.75	10/8

The bunch rotator is needed primarily for the short-bunch mode that is to be implemented on a lower priority. The 503.125-MHz buncher is not needed at all for long-bunch operation. Programmed injection steerers, nonlinear correction magnets, and a damper may be needed for achieving reliable low-loss operation at the 100-μA level and will be implemented, if required, by the end of 1986.

Some additional assumptions underlying the tuning plan are that

- all other PSR equipment will have been checked out and will be operational at full design specifications;
- there will have been early "first beam" tests (April) that allowed attainment of an initial closed orbit;

- the H^- beam transport to the ring will have been tuned and optimized;
- Line-D to Weapons Neutron Research facility (WNR) target operations will have been restored;
- multiplexed operation between Line-D and the PSR injection-line will have been achieved;
- beam currents below 100 nA can be safely dumped in the ring, but above this level, extraction to the tune-up beamstop is necessary;
- tune-up runs will be scheduled as several-day intensive study periods, staffed around the clock by PSR design staff and a WNR operations crew.

SETTING THE CORRECT B-FIELD AND INJECTED MOMENTUM

A particular problem during initial setup of the ring is the correct determination of the average ring radius (R), the beam momentum (p), rf buncher frequency (f), and the ring bending magnetic field (B). At this time, the momentum of the LAMPF beam is not normally controlled to better than a few MeV in 800 (0.5%). However, correct operation of the PSR bunching systems will require that momentum be set to within ±0.1%. Taking note of the dynamic relations between the four quantities (R, p, f, and B) and assuming R and f to be primary standards (or constants), we have derived a simple scheme for producing correct settings for B and then p during initial beam tests. The scheme calls for temporary adjustment of the ring quadrupole strengths to set the lattice transition energy at the beam energy.

After inital setup, B will be held to the desired value by a nuclear magnetic resonance (NMR) probe in a PSR dipole and, secondarily, by regulation of the dipole energizing current. Injected beam momentum will be actively regulated by a feedback signal that adjusts the phase of the last accelerator rf module (48). The signal is derived from a high precision time-of-flight (TOF) measurement based on phase comparison of the 201.25-MHz reference and micropulses detected at two stations in Line-D, separated by 100 m.

THE TUNING PLAN

Following establishment of the correct B and p, the ring closed orbit will be measured and corrected using the 17 BPMs located inside the quadrupoles, a computer program that calculates the necessary quadupole offsets and dipole rotations, and then appropriate manual adjustment of these elements will be done. The procedure may require two or three iterations to converge. Two of

the quadrupoles are to be motor driven to allow "on-demand" distortion of the normal closed orbit for diagnostic purposes.

After these inital steps, we envisage a program of progressive steps in which the PSR injection, bunching, and extraction operations will be carefully studied and brought up to specification. Average beam currents will at first be kept low (<100 nA), using short accumulation times and low repetition rates, to allow beam to be dumped in the ring witnout inducing serious activation levels. After we have brought the extraction system into operation, the tune-up beamstop located beneath the extraction channel will be used, and tuning beam currents can increase. By late August, we expect to be able to raise peak current levels into the region where space-charge effects are significant, and to begin studying tune spreads and beam dynamics under these conditions. By October, about 20-μA (average) beam currents should be available for WNR experimenters. We imagine a schedule in the last quarter of 1985 in which the PSR runs 70% of the time at this level for users and the remaining 30% for continuing commissioning studies.

During the fall of 1985, as peak-current levels are raised toward the PSR design goals, various difficulties related to space charge can be expected to appear (between 5×10^{12} and 5×10^{13} protons accumulated). We then hope to evaluate the need for implementing passive and/or active correction elements (sextupoles, octupoles, fast transverse damper) whose construction has been deferred because of funding limitations.

The final target for the long-bunch mode is to have a reliable 100-μA beam on the neutron-production target by the end of 1986.

The short-bunch mode, assigned lower priority during PSR construction, will begin tuning in 1986. Installation of all equipment needed for this mode is expected by April 1986, with earlier inclusion (September 1985) of one set of the 500-MHz cavities in the ring to allow evaluation of their effect on the longitudinal charge distribution in the long bunch. Initial operation of the ring in short-bunch mode is planned by May 1986, with tune-up to full current by September 1986.

MAGNET MAPPER

A precision magnet mapper was constructed as an AT-Division facility for measuring the field distributions of dipole magnets. The mapper's first application was to determine the quality of the PSR ring dipole magnets. These 36° bending magnets confine the stored beam in PSR to a definite trajectory for up to ~5 000 turns. Imperfections in their fields tend to destabilize particle motion with a subsequent undesirable increase in beam size and beam spill. We developed criteria that are sufficient to reduce such destabilization to a negligible amount. These criteria require

- the effective magnetic lengths to be the same for all 10 dipoles to within 1 part in 10^4,
- the integrated sextupole field of each magnet to be less than 10^{-4} of the dipole field, and
- the magnet-to-magnet variation in the end-configurational lens strength to be less than 10^{-4} of the ring quadrupole strengths.

These quantities can be adjusted by appropriate machining of removable pole end blocks and are determined from the field map. For this application, measurement accuracy of a few parts in 10^5 are required.

INITIAL PERFORMANCE

The mapper performs measurements by monitoring the voltage induced in a small-diameter coil passed longitudinally through the aperture of the magnet with its axis parallel to the dipole field direction. The coil voltage is converted to a frequency that is counted, integrated, and calibrated against an NMR standard. Corrections are made by a data-acquisition computer (LSI-11) for voltage/frequency conversion nonlinearity and drift. Because the mapper both counts and integrates using the same (precise) time standard, high precision in coil velocity is not required. Rather, precision in coil tracking, careful calibration, and good system alignment, as well as temperature stability, determine the accuracy obtained. A great deal of care was taken in mechanical design, bench calibration, and software processing to effect the desired high accuracy.

Nevertheless, the initial application of the mapper to PSR dipole measurements (its first task) indicated that it was not adequate to produce maps with an accuracy of better than one part in 10^3. Consequently, a concentrated and

dedicated effort was mounted to identify and correct the problems and to increase the mapper measurement accuracy to the required level. A four-man team drawn from the Division's storage-ring- and magnet-technology groups implemented the improvement programs, and the effort applied was intense.

Several effects were found that influence the measurement accuracy, and changes were made to obtain improvements. The highlights are listed below.

- Temperature sensitivity: After extensive investigation, several temperature effects were isolated and measures were taken for their elimination. A constant-temperature oven now houses the analog electronics that processes the sensing-coil signal, and the effects of varying coil resistance and size have been balanced out. A residual combination of complex temperature effects remains, which is corrected in software and has been minimized by enclosing and air-conditioning the entire mapping area. Removal of these temperature dependencies constitutes the greatest single improvement in mapper accuracy.
- Analog electronics: A new measuring-head electronics package was constructed with improved line isolation, circuit configuration, and decreased microphonic sensitivity. Improved linearity and stability is desirable but may only be achievable by rather elaborate reworking of the inherently noisy voltage-to-frequency conversion process.
- Diagnostic and procedural software: Several generations of computer programs have been written to help in our diagnosis of mapper problems. A series of complex programs has been written that transforms results from the linear mapper scans to the curved magnet coordinates and performs harmonic analysis. Additionally, a DECNET link from the mapper control computer to the PSR VAX controls computer has been set up. This link will facilitate data transfer and provide rapid feedback on mapper performance to the operator.
- Coil alignment: The electrical and mechanical axes of the mapper coil apparently do not coincide. Large contributions to the measurement error are thereby made by sensing field components orthogonal to the desired direction. An electronic alignment fixture was constructed that has microradian resolution and permits coil alignment to within the milliradian required.

- Internal correlations: For a particular mapper probe trajectory (one pass in and out), the measured fields are not exactly the same entering a magnet as exiting. The magnitude of this difference ($\sim 1/10^4$) varies randomly for successive scans and demonstrates a complex dependence on the (x-, y-) position within the magnet. The effect appears to be caused, in part, by mechanical tracking errors of the probe carriage and, in part, by small imprecisions in the amplifier-gain calibration. For a particular scan trajectory, we can obtain and empirically correct the data to a reproducibility of $1/10^5$. The appropriate procedure is now being established for matching scans of the multiple trajectories required to produce a complete multiplane map.

- Power supply: The PEI power supply purchased to energize the 10 ring dipoles in series has been used with a secondary tap to map single magnets. The magnet current contains substantial ripple in this configuration. To remedy this, we have obtained and installed a high-current low-pass filter on the power-supply output. We have also implemented a computer-controlled schedule for cycling magnets to enhance field reproducibility.

RESULTS

As an example of a mapper scan, Fig. 4 shows a plot of magnetic field (in the PSR dipole prototype) versus distance along a scan. The peak at z = 100 cm seen in the magnified view is spatially associated with the locations of the magnet support posts, and the rise in field at the end corresponds to passage of the probe above the magnet shims. The magnet center near z = 170 cm shows a local minimum.

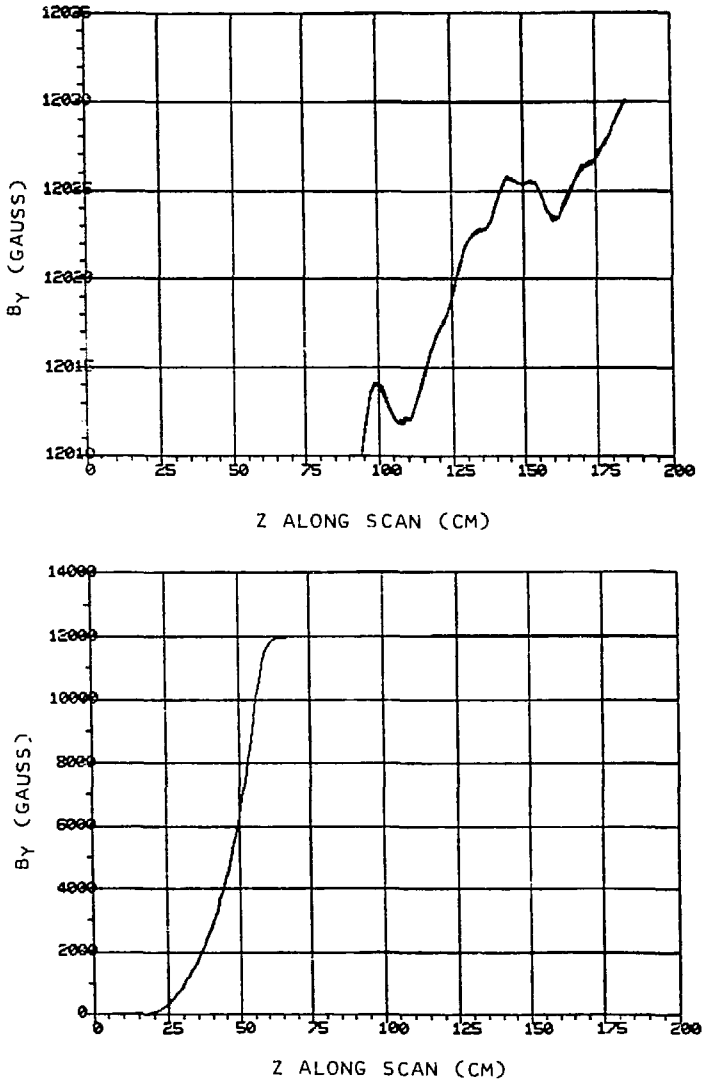

Fig. 4.
Plots of magnetic field versus distance along a linear mapper scan through the PSR prototype dipole. The scan extends from outside the magnet to past the longitudinal center. The top plot is a magnified (X 560) view of the "constant" field region in the lower plot.

The form of a final map is shown in Fig. 5 as a list of harmonic coefficients and a plot of the effective field lengths for half the magnet, calculated along trajectories that are parallel to the nominal particle orbit through the magnet center. In this plot, the linear dependence (representing a configurational end lens or quadrupole term) has been subtracted from the results so that the symmetry of residual harmonics may be seen.

```
DIPOLE IS   127.485088345 CM
'QUADRUPOLE' FRACTION IS   8.604208771B3E-04
SEXTUPOLE FRACTION IS   1.690487879J4E-04
OCTUPOLE FRACTION IS   2.403276012S2E-04
DECAPOLE FRACTION IS   3.734677640J2E-04
DUODECAPOLE FRACTION IS   5.88983457460E-05
```

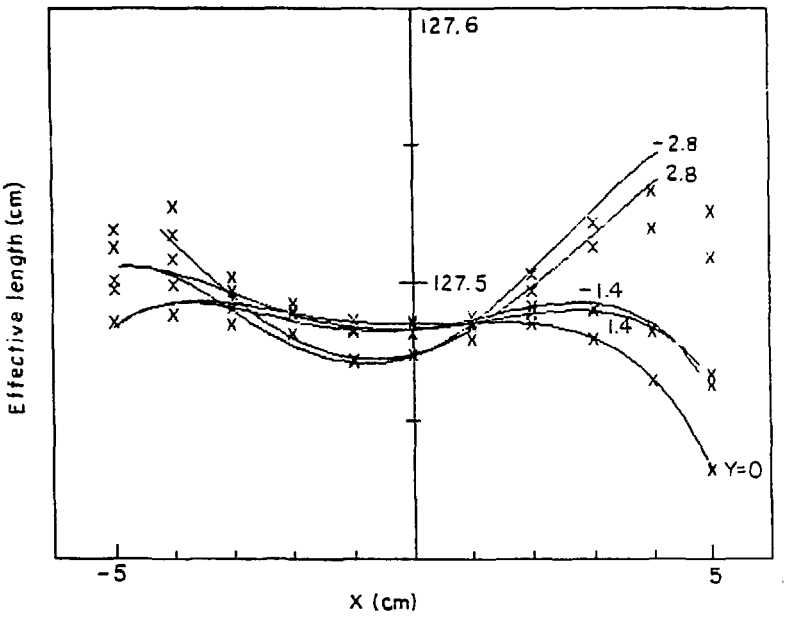

Fig. 5.
Listing of the harmonic decomposition for a half-magnet map and a plot of the integrated field (normalized to the mid-plane field and, hence, representing an effective length) parallel to the central particle orbit (x = 0, y = 0) through the magnet. The linear (quadrupole) part of the decomposition has been subtracted. The asymmetry about x = 0 is configurational and not an error in mapper coordinate assignment. The y-values for each of the five separate plane scans are indicated on the right.

PSR MAGNETS AND POWER SUPPLIES

Significant progress toward procurement of these major PSR components was made during the reporting period. We now have on hand at Los Alamos 6 (of 11) ring dipoles, 13 (of 21) ring quadrupoles, all but 2 of the injection- and extraction-line quadrupoles, and all but 1 of the injection- and extraction-line dipoles. All the magnets in the injection line and the quadrupoles in the extraction line have been mounted in position. All other magnets are on order, with the exception of the two ring extraction septa, the H° stripper magnet, and the injection- and extraction-line steering magnets (Fig. 6).

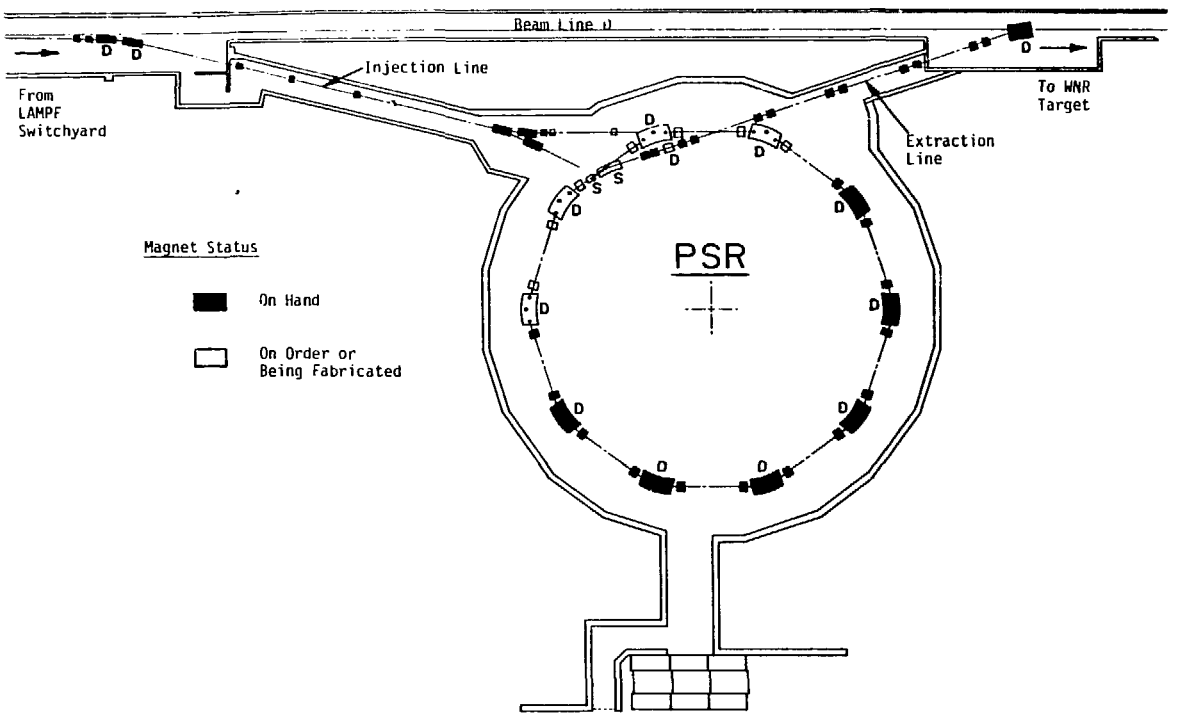

Fig. 6.
Proton storage-ring layout highlighting magnet status.
D = Dipole magnet
S = Septum magnet
No label = Quadrupoles

Power supplies for the ring dipoles, all injection-line magnets, and extraction-line quadrupoles are on hand. All others are on order, with the same exceptions as noted for magnets above.

Some effort was put into adding a filter to the main ring dipole power supply (a 12-phase 605-kW SCR unit) to eliminate 720-Hz ripple. The power supply was also interfaced to an LSI/11-CAMAC control unit to provide automated cycling of the dipole current on the measurement test stand—an operation that requires an hour to complete. Addition of the filter also has permitted satisfactory operation of the NMR field reference that is used as the flux standard during mapping.

Harmonic field-component measurements on the four unsatisfactory 4-in. extraction-line quadrupoles showed that three units had a coil with one turn less than normal and one unit had a coil with one extra turn. We removed two turns from the latter and, together with the other three, produced a balanced coil set with acceptable characteristics for one quadrupole. All four quadrupoles now meet the specifications; Table III shows the field-harmonic measurement results before and after correction. The prototype 7-in. quadrupole for the ring was measured and shimmed; Table III also shows the results after shimmering. The quality of all the quadrupoles is now satisfactorily high.

The septum magnet for the LAMPF switchyard has been prototyped and measured in a 1-ft-long, full cross-section model. The results are satisfactory. Final drawings have been made, and the full-length production magnet is being fabricated. Drawings for the first ring extraction septum are complete except for some vacuum pipe and support details.

Magnets provided for Line-D portions of the PSR extracted beam path include eight 6-in.-bore and four 4-in.-bore quadrupoles. On order for the upgrade of the north end of Line D are four quadrupoles and three 4-in.-gap dipoles. Preliminary design work has been done on the transport-line steering magnets and 4-in.-bore, radiation-hardened quadrupoles to be installed above the upgraded WNR target.

TABLE III

QUADRUPOLE HARMONIC MEASUREMENTS

	Extraction Line, 4-in. Quadrupoles		Ring, 7-in. Quadrupoles
Harmonic Type	% Harmonic Before Repair	% Harmonic After Repair	% Harmonic
Sextupole	0.14	0.046	0.076
Octupole	0.039	0.025	0.05
Decapole	0.01	0.007	0.02
Duodecapole	0.027	0.045	0.027

The 503.125-MHz BUNCHER

The buncher system for the PSR short-bunch mode consists of four pairs of LAMPF-style side-coupled cavities operating at 503.125 MHz. Fast tuning to compensate for variable beam loading is accomplished by a ferrite-loaded rectangular TE_{01} cavity that is resonantly coupled to one of each pair of bunching cells.[1] The ferrite is biased perpendicular to the rf magnetic field in the tuner, enabling high-Q operation over the required 200-kHz tuning range. An aluminum cold model of a complete buncher unit (two bunching cells, side-coupling cell, tuner, and tuner coupling cell) was built to determine coupling constants, mode behavior, and tuning operation. Detailed measurements were made.

The data were used in a computer program developed to determine the cavity mode frequencies as a function of tuning-cavity frequency. Changes in the model parameters are necessary to achieve the desired tuning range without having any mode of the five-cavity system approach too closely to a PSR beam-harmonic frequency. A computer program was developed to determine the effective shunt impedance of the cavity modes as a function of frequency.

The geometries of the ferrite tuning cavity and the adjacent coupling cavity were changed to obtain a sufficiently large coupling constant (7.4%) at the proper frequency.

Posts were introduced into the buncher cavities to test a scheme for reducing the Q of the cavity deflecting modes while leaving the Q and frequency of the bunching mode unaffected. Results of these tests showed that (1) the posts would have to be oval in cross section in order not to affect the bunching mode frequency, and (2) because of the oval cross section, the Q of the bunching mode would be significantly lowered.

PSR EXTRACTION KICKERS

The PSR extraction kickers are designed to operate in two modes, corresponding to the two operating modes of the ring. In the long-bunch mode, a single 270-ns bunch is extracted every 83 ms. In the short-bunch mode, six 1-ns bunches are extracted at 1.4-ms intervals every 8.3 ms. (This corresponds to a continuous rate of 720/s.) The two kicker magnets, which are located in Ring Sections 7 and 8, must coherently deflect individual bunches into the extraction line without disturbing remaining circulating bunches. This deflection imposes extreme requirements on the rise time, fall time, and after-pulse

ring out of the kicker fields, which has led to a system design using strip transmission-line deflectors.[2] The two transmission-line electrodes in each kicker are driven with pulses of opposite polarity, generated by high-voltage modulators that are thyratron-switched, ferrite-isolated, Blumlein pulse-forming networks (PFN).[2,3] These PFNs are charged through an intermediate storage capacitor and a 1:10 step-up transformer. The required pulses have voltages of ±45 kV, with strict tolerances on flat top and jitter.

The design and development of the kicker modulators has been a challenging several-year project that now is essentially completed to specifications. A typical PFN output pulse for the long-bunch mode is shown in Fig. 7. The picture was taken with a sampling scope. There is very little time jitter from pulse to pulse. The rise time is sufficiently short and the pulse is sufficiently long and flat for long-bunch operation.

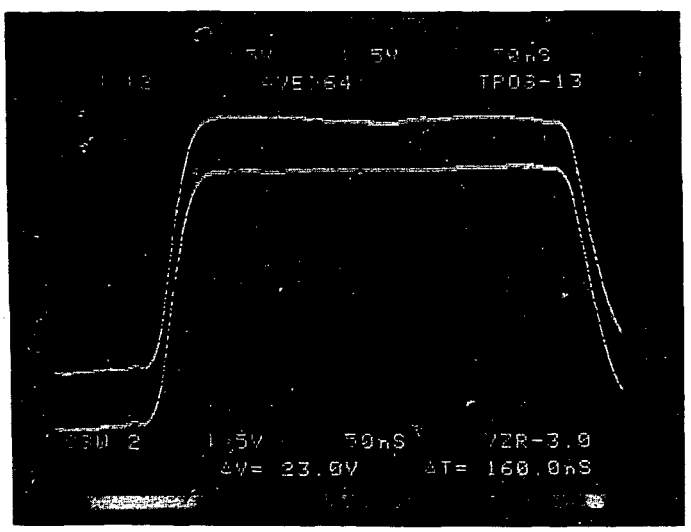

Fig. 7.
Long-bunch mode kicker-modulator output. Pulse-height is 50 kV; time scale is 50 ns per division.

The design of the two pairs of kicker electrodes recently has been finalized. Each pair of plates is 3.95 m long; a typical cross section is shown in Fig. 8. The distance D is tapered along the electrodes to minimize the required pulse voltage. The exact shape of the plates is dictated by field quality requirements and impedance considerations. With a constant angle α, a height H that is tapered along the electrodes, and an edge length L that varies with position along the electrodes, deflection fields having sextupole components of less than 2% of the dipole field can be obtained. The bare

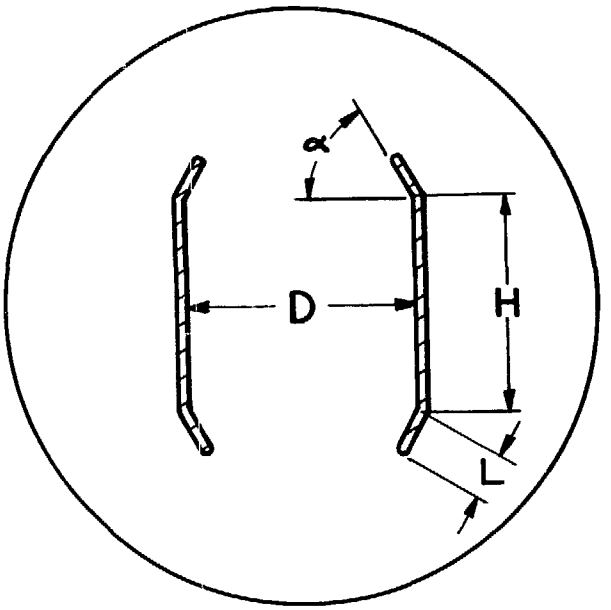

Fig. 8.
Cross section through kicker electrodes and vacuum pipe. The critical dimensions in fabrication are the shim angle α, shim length L, and plate center-section height H.

transmission-line impedances along the plates vary between 52 and 60 Ω; these will be adjusted to a uniform value of 50 Ω by impedance-lowering structures attached to the rear of the plates.

Plate manufacture will proceed in two steps: bending of the plates to the correct angle α will be done by a commercial machine shop with a long sheet-metal break, and milling of the edges will be done on a numerically controlled milling machine (Mazak) in AT Division. The data files for this machining operation have been produced.

The electrodes of the first kicker (Ring Section 7) are inside an 8-in.-diam pipe; those of the second kicker (Ring Section 8) are inside a 10.5-in.-diam pipe. Both are on hand and inspected. Flanges and bellows are ordered or are on hand. Because of the horizontal separation between the stored beam (unperturbed) and the kicked beam, oversized vacuum pipes are needed through the dipoles and quadrupoles Ring of Sections 7 and 8. The diamond-shaped vacuum pipes needed for beam clearance in the two focusing quadrupoles in these sections are on hand and leak checked.

The drafting effort is largely completed, including an approved design of the adjustable supports for the kicker electrodes (Fig. 9).

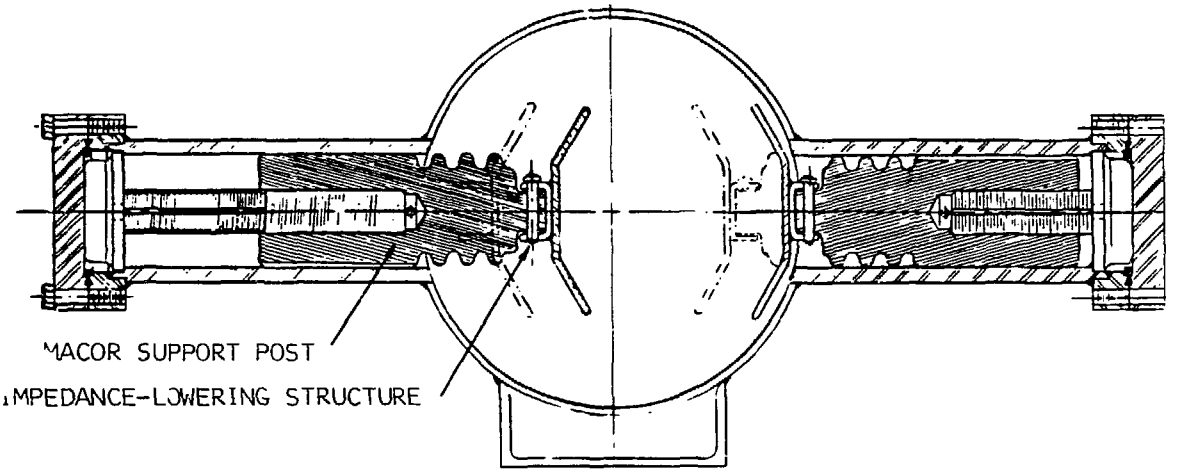

Fig. 9.
Cross section of the kicker-plate supports and impedance-lowering structures.

The electrodes are scheduled to be completed by mid-July 1984; installation of the kicker components in the ring tunnel and the PSR equipment building will take place from June to November. The period from the end of November to mid-February 1985 is reserved for testing of the entire system.

BEAM-POSITION MONITOR SYSTEM

The Beam Position Monitors (BPMs) are the primary diagnostic devices for steering beam through Line D and PSR transport lines and for determining positional errors of the circulating beam in the ring. The system has been described previously in PSR Technical Note 36, in Ref. 4, and in previous AT-Division progress reports.

During this reporting period, several major parts of the BPM system have been completed and are being installed. Final integration of the system is proceeding with a goal of actually monitoring beam through three sensors in Line D during the upcoming LAMPF run cycle. This will provide an outstanding opportunity to test the system and to work out problems nearly a year before PSR turn-on. Each major design area and its status is described briefly below.

Beam Sensors

There are about 60 beam sensors being installed at strategic locations in the LAMPF switchyard, along Line D, in the PSR injection and extraction lines, and in the ring itself. Each unit consists of four strip-line electrodes arranged in quadrature and spaced from the wall to give 50-Ω characteristic impedance. The vacuum housing, electrodes, and ceramic feedthroughs must be carefully shaped to achieve good impedance matching and smooth transitions in the inner wall seen by the beam. This requirement led to a rather complicated structure in which the electrodes are placed in longitudinal recesses on the inside of the vacuum housing. Because of the large number of sensors required, the cost of fabricating these structures became a major concern. After machining an expensive prototype, we found an explosive-forming technique whereby the vacuum housings could be manufactured at a considerable cost savings ($440/unit compared to about $3500). Including the die cost, terminators, and other manufacturing costs, the sensor fabrication costs ranged from $2400-$2800 each, depending on the type. Guiding the BPM sensor production through explosive forming of housings, welding of flanges and feedthroughs, accurate positioning of electrodes, cleaning, leak checking, and calibration of the electrical center line to within ±0.2 mm has been an extensive process, now nearing completion. About half of the units are ready for installation and the remainder will be finished within 2 months. The electrical-center calibration data have been inscribed on the flanges so that the monitors can be installed with zero offset from the desired beam trajectory. PSR Technical Note 126 has been drafted to document the calibration procedure.

Beam-Position Processor

The signals coming from the BPM sensors are detected and analyzed in two processors (vertical position and horizontal position) using a phase-type differential correlation technique. The dynamic range of 26 dB (factor of 20 in beam intensity) allows for tracking position within the storage ring as intensity increases during an injection cycle. Switchable gain extends the overall range to 46 dB (factor of 200). Thus, the system is capable of determining beam position for a single LAMPF micropulse (3×10^8 protons) up to the full intensity in a PSR short bunch (1×10^{11} protons). For the PSR long-bunch mode, the processors look in the injection transport system at the 200-MHz component of the H^- pulse string from the linac. In the ring, they examine the

200-MHz component of the complex signal that develops as the accumulation process advances. In the extraction channel they look at high-intensity noise-like signals. The system dynamic range, switchable gain, and programmable attenuators are designed to handle this variety of signal inputs. The processors have been completed and tested using both simulated signals and beam-induced signals from a prototype sensor installed in the LAMPF switchyard. Using a nearby wire scanner as a standard, the prototype system was found to be accurate to about 0.25 mm in measurement of beam position, with comparable stability over a 6-day period.

Multiplexers

To keep system costs down, we decided to use multiplexers to couple the filtered beam signals from selected sensors to single processors for each measurement plane. The multiplexers are digitally driven rf switches that are arranged in two groups. The first group (10 channels) consists of high-power low-loss relay switches that select 1 of 10 transport-line or storage-ring zones. Individual sensors within each zone are then selected by groups of 8 relay switches or groups of 12 solid-state switches. The solid-state switches are used with the injection transport sensors, where signal levels are low and dynamic-range requirements are not large. The three racks of multiplexer units have been completed and are ready for installation.

Cables

The cable plant for the BPM system consists of about 240 high-quality low-dispersion coaxial cables to carry signals from sensors to the multiplexer units. Phase matching of each pair is required so that the detected signals will arrive simultaneously at the analog processing equipment. The specification is that each cable pair will be phase matched to within 2° at 200 MHz after the connectors have been installed. Two separate operations are required. First, a propagation time measurement is made that enables the operator to cut the two cables so that they are electrically within the same wave period. Second, the phase is matched exactly using an oscillator and vector voltmeter. PSR Technical Note 124 has been written to document the phase-matching procedure. About half of the cables have now been installed and terminated, with the remainder (primarily the shorter cables going to the ring sensors) to be completed in August, 1984.

Digital Control and Interfacing

The analog-position signal selected by the multiplexer unit is applied to a track-and-hold gate and an eight-bit analog-to-digital converter (ADC). Timing information to trigger the sample circuit can be selected from four sources: (1) a beam-present signal coming from the analog processor, a so-called "self trigger"; (2) a beam-trigger receiver that detects beam bursts entering the PSR injection line; (3) the 2.8-MHz synchronization signal for beam circulating in the ring; or (4) the extraction trigger used for kicking beam out of the ring. In addition, an overall timing delay can be applied to start data acquisition at some point after the beginning of an injection cycle. A microprocessor system controls the timing and sequencing of data acquisition and communicates to the VAX control computer with CAMAC I/O units. This part of the system was described in the previous AT-Division status report and is now being completed. Initial communication tests with the VAX have proved the control and data transmission procedures. Final timing and integration tests are currently under way.

Computer Program

The VAX computer program for control and display of the BPM system has been completed and tested. The program is menu driven from a color touch-panel control screen, and overlay screens are provided to display the data in several formats. We believe that a high degree of flexibility is built into the program for display of information from selected sets of monitors. It can also be operated very simply to acquire and display a single monitor output. Figures 10-13 illustrate several of the display screens.

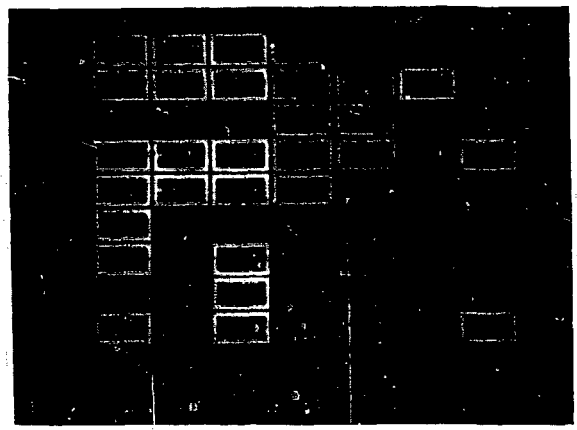

Fig. 10.
The BPM system main menu. The first three columns allow detector area selection with choice of start and end channel or an arbitrary list of up to 20 channels. The other columns set up general parameters, cycle control, type of data display, and timing functions. The numeric keypad appears when certain parameters are changed.

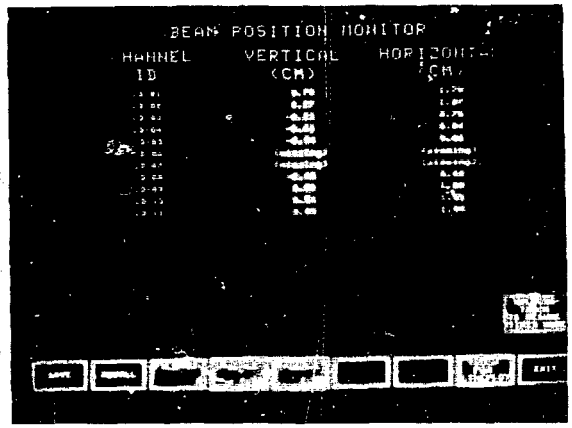

Fig. 11.
Alphanumeric data display for the channels and parameters selected on the main menu. Touch panels at the bottom allow selection of other displays or freezing the display during continuous data acquisition.

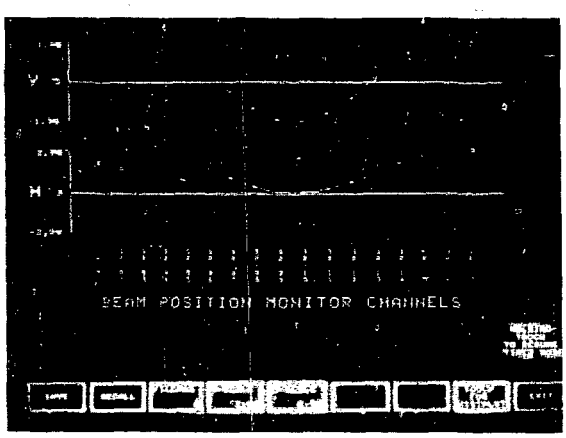

Fig. 12.
Position data display for selected channels as a function of BPM location. This line display connects adjacent locations to give a representation of beam trajectory. Use of color and broken-line segments flags channels where no data are present. SAVE and RECALL touch buttons allow overlay of different trajectories.

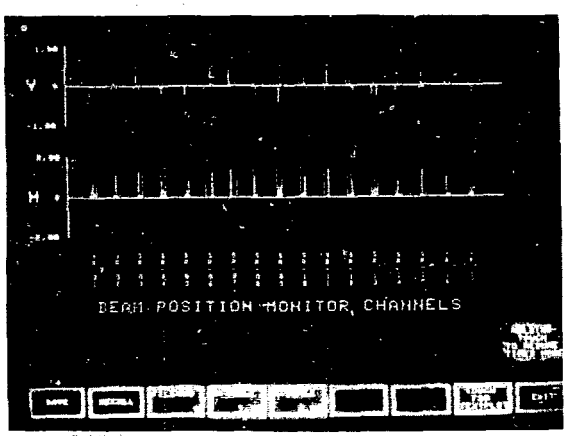

Fig. 13.
The data can be displayed in a histogram mode that includes the last five readings at each BPM channel position. Scale factors can be changed by touch buttons on the screen. The EXIT button on any display screen returns to the main menu.

REFERENCES

1. D. W. Hudgings, and A. J. Jason, "Los Alamos Proton Storage Ring Extraction System," IEEE Trans. on Nucl. Sci., NS-28 (3, Part 2) 2791, (June 1981).

2. W. C. Nunnally, D. W. Hudgings, and W. J. Sarjeant, "Fast-Extraction Modulators for Los Alamos Scientific Laboratory Proton Storage Ring," Fourteenth Pulsed-Power Modulator Symp. Orlando, Florida, June 3-5, 1980, 292, (1980).

3. J. F. Power, W. C. Nunnally, K. R. Rust, J. S. Samuels, and G. Spalek, Fast Extraction Modulators for the Los Alamos Proton Storage Ring," Proc. 4th IEEE Pulsed Power Conf. Albuquerque, New Mexico, June 6-8, 1983, 263, (1980).

4. E. F. Higgins and F. D. Wells, "A Beam Position Monitor System for the Proton Storage Ring at LAMPF," IEEE Trans. on Nucl. Sci. NS-28 (3), 2308 (June 1981).

H^- ACCELERATOR PROGRAM

ION SOURCE DEVELOPMENTS

Small-Angle Source

The H^- small-angle source (SAS) was installed on the accelerator test stand (ATS) during this period. Tests of the 100-keV beam occupied much of the ATS running time. On the ion source test stand (ISTS), the SAS had produced as much as 180-mA H^-. Emittances measured at 20 keV on the ISTS were 0.004 π•cm•mrad in the x-plane and 0.027 π•cm•mrad in the y- or bend-plane, both normalized rms values. On ATS, a maximum of 130 mA has been transported to the RFQ match point with measured emittances at 100 keV of 0.011 π•cm•mrad in x and 0.024 π•cm•mrad in y.

Beam neutralization appears to exercise a dominant effect upon emittance growth experienced on ATS. On the ISTS, variations in neutralizing gas density appeared to have little or no effect on measured emittance areas. On the other hand, measurements on ATS at 100 keV show a marked sensitivity to beam neutralization. A partial answer to this effect can be found in the observed coupling to third-order aberrations in the accelerating column, which is minimized by proper neutralizing gas (xenon) flow. Noisy arc conditions (as occur during source conditioning), which produce beam-current fluctuations, render stable neutralization difficult and lead to strong emittance growth.

Routine, quiet arc operation (noise = $\leq$ 5%) of the source has been attained on ATS and, with the flow of neutralizing gas adjusted properly, the SAS is a more-than-adequate ATS injector.

Scaled Circular-Aperture Ion Source

Circularly symmetric beams could be matched more easily into the RFQ acceptance than the output from the SAS with its highly asymmetric slit (0.5- by 10.0-mm) geometry. In addition, the cathode power loading of the SAS (7-16, kW/cm^2) renders dc operation unfeasible. A circular-aperture Penning surface-plasma source, scaled to reduce cathode power loading, has been constructed. This source eventually could replace the SAS on ATS, and a study of its operating characteristics will test our understanding of the scaling laws applicable to these ion sources.

Initial tests have been performed on the ISTS. The source has been operated in two modes. A mode with noisy arc conditions (±45%) has produced 90 mA H^- within an emittance of 0.017 π•cm•mrad x 0.022 π•cm•mrad. Quiescent arc operation (noise = ≤ 1.5%) has produced 40 mA with an emittance of 0.007 x 0.008 π•cm•mrad. Studies of methods of producing quiescent arc operation at increased current are continuing.

ATS LOW-ENERGY BEAM TRANSPORT

Beam-transport studies of a relatively long (1.7-m) LEBT section revealed unacceptable emittance growth in the 100-keV region. The beam-transport region before the RFQ has been reduced to less than 0.875 m, including the 20-keV region and the accelerating column. This reduction in length dictated the development of a compact lens system capable of matching the ion source output into the RFQ acceptance. Such a system has been constructed using compact rare-earth cobalt (REC) quadrupole elements.

The transport and matching elements consist of four quadrupole-magnet singlets. Match parameters were measured approximately 7.5 cm before the RFQ match point, using an emittance miniscanner developed in AT Division. Required variations in focal strength of the system were obtained by physically repositioning the elements. Figure 14 is a TRACE output showing the beam envelope through the system and a comparison between the match obtained and the RFQ acceptance. This is probably the most compact system ever used to transport the beam and obtain required RFQ match parameters.

ATS RFQ

Tuning Procedures and Results

The ATS RFQ was reassembled after vane remachining, during which it was retrofitted with vane coupling rings (VCRs), an innovation of Lawrence Berkeley National Laboratory. Originally it was fitted with seven complete VCR pairs located at the λ/2 points in the structure. Because the shift in operating frequency (caused by the capaciti oading that is due to the rings) was considered excessive, a configurat consisting of alternating horizontal and vertical VCRs was investigated. When vane misalignments were held to ±0.05 mm, relatively easily obtained mechanically, this arrangement reduced dipole

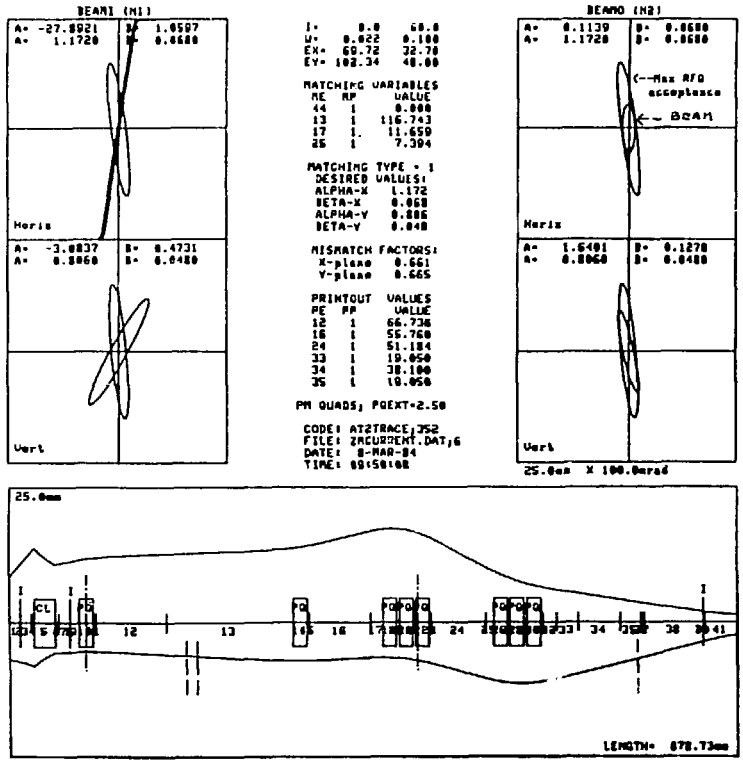

Fig. 14.
TRACE output showing the beam envelope through the system and a comparison between the match obtained and the RFQ acceptance.

components in the RFQ field to less than 4%. Final tuning was accomplished using the alternate ring concept.

In tuning the longitudinal field distribution, it was found necessary to increase the capacitive loading of the ends (beyond the point possible with a standard end-tuner arrangement) without an unacceptable increase in the sparking probability. A redesigned end tuner in which copper slugs are inserted into the quadrants between the vanes provided the necessary end capacitance.

Figure 15 shows the final longitudinal distribution of the quadrupole field in the RFQ and also shows the total dipole content of the field. This field was used as input to a modified version of PARMTEQ (see Theory and Simulation below). Little difference in performance from that predicted for an ideal field distribution resulted.

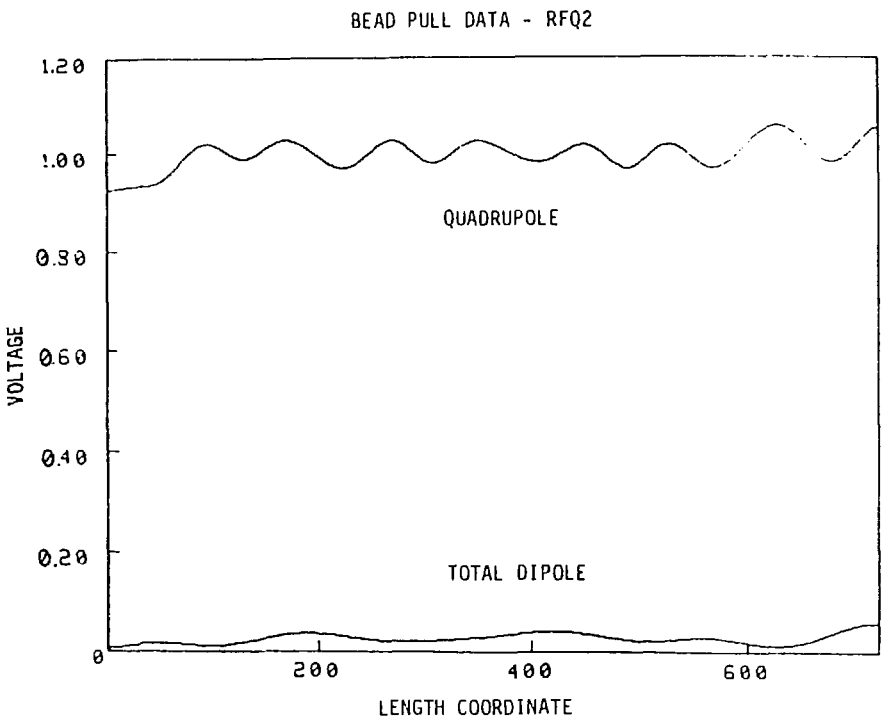

Fig. 15.
Final longitudinal distribution of RFQ quadrupole field and total dipole field.

RFQ Operating Results

The RFQ was installed on ATS and went through a normal rf conditioning process. On February 22, 1984, beam was first accelerated to full energy and on March 20, 1984, 95-mA of H^- was accelerated after revising the input-matching lens system. Figure 16 shows the observed transmission as a function of vane voltage for the initial input match compared with that calculated with PARMTEQ—the agreement is good. In Fig. 17 are shown preliminary measurements of the output energy distributions, again compared with PARMTEQ predictions.

Investigation of RFQ operating parameters and experiments to fully characterize the output beam are just beginning. In addition to the output spectrometer and standard emittance-measuring stations, a 25-ps pulsed laser has been installed to aid in measuring longitudinal emittance characteristics.

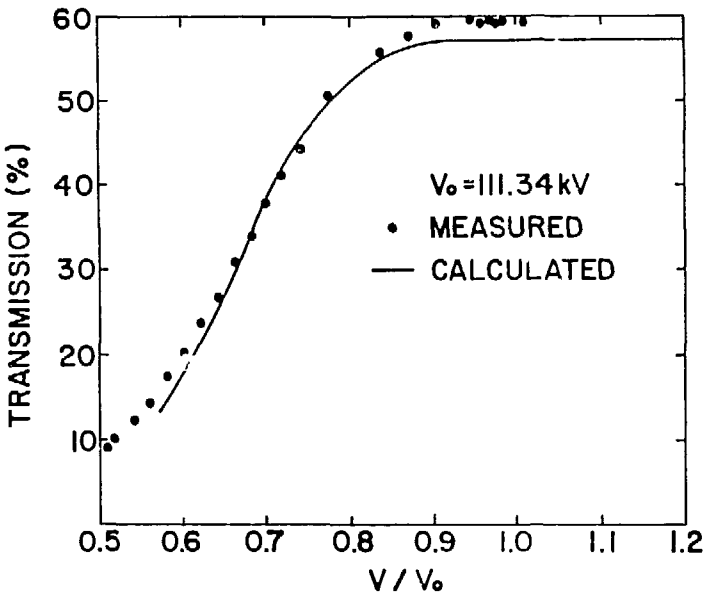

Fig. 16.
Observed transmissions as a function of vane voltage for initial input match compared with PARMTEQ calculations.

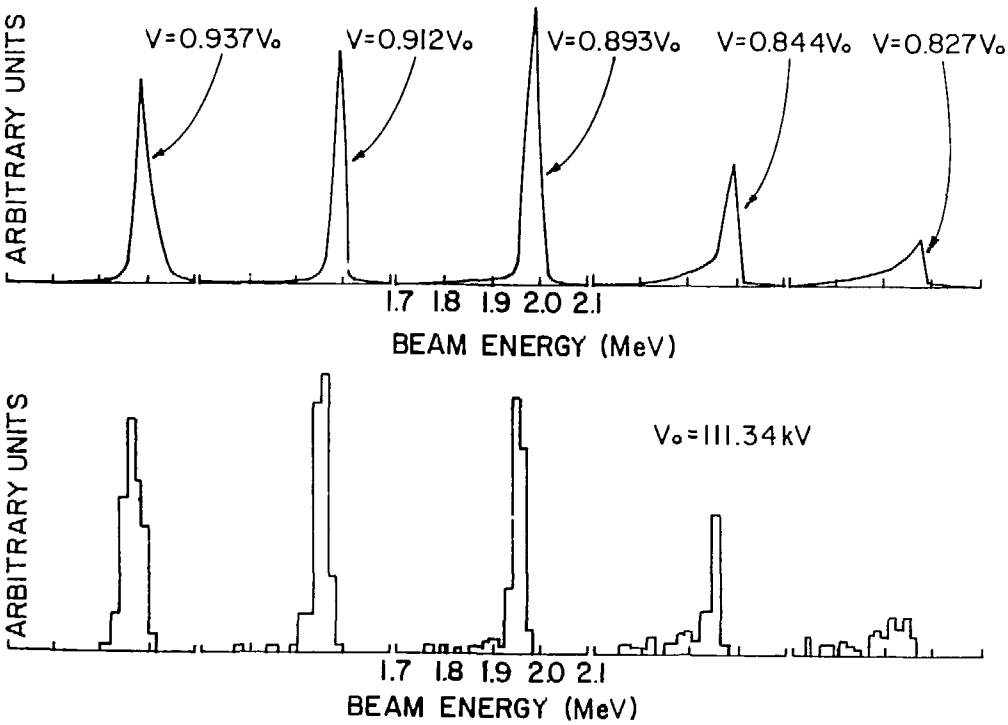

Fig. 17.
Preliminary measurements of the output energy distributions compared with PARMTEQ predictions.

THEORY AND SIMULATION

Beam Dynamics

PARMTEQ. This code has been modified to incorporate the parameters of the measured RFQ field distributions and geometry. The version in current use is restricted to fixed-frequency (that is, design-frequency) simulations but agrees quite well with measured results. A further refinement, allowing time-dependent calculations, is being modified to accept both measured RFQ parameters and measured input particle distributions. This modification will allow even more precise comparison with experimental measurements to test the accuracy of the simulation.

RFQ Design Codes. The Division has continued work upon a generalized RFQ design code based upon structured programming techniques. This work is based upon a program library, RFQLIB,[1] which makes it relatively easy to generate new design codes with their necessary documentation. The standard version of the simulation code in RFQLIB is RFQRZP, which is a particle-in-cell code using an r-z Poisson solver to perform the space-charge calculations. Current results, where tested, are very similar to those obtained from PARMTEQ.

ACCELERATOR THEORY AND SIMULATION

CODES

SUPERFISH

The present VAX version of SUPERFISH has been brought up on CTSS. The code has been partially reconfigured to allow very large problems (greater than 40 000 mesh points) to be run. All changes have been made in such a way that the code can be transferred back to the VAX system by minimal use of a text editor. Complementary versions of the output routines TEKPLOT and SF01 have also been brought up under CTSS.

ULTRAFISH

R. L. Gluckstern, Laboratory consultant, has provided equations for a second version of ULTRAFISH. The dependent variables in this formulation are E_2 and rE_r. The new system does not suffer from the $\hat{r}$ singularity to which the original version was subject.[1] During this period, work with the new code has shown that one of the metal boundary equations produces a numerical instability that prevents the root finder from working properly. The offending equation has been replaced and the code reprogrammed, but still requires further testing.

Two other programs have been completed and debugged. One, named COST, calculates the cost of synchrotron magnets, chokes, power supplies, and condensers. The instructions for using this program are written. The cost program requires beam size, etc., for input. These sizes are calculated by a program named SIZE. This program will limit the Laslett tune shift if this is required. The program is debugged and the instructions are being written.

Additional codes during this reporting period have been updated and implemented on our computers are discussed below.

TRANSPORT

The latest FTN modified version of A. Paul's TRANSPORT, a code for the evaluation of charged particle beam-transport system, is now available on LTSS. Modifications have been made to correct a number of errors that A. Jason (AT-3) found and that A. Paul concurred were oversights. This version has also been augmented to generate an additional file, TAPE3, of output and plots that are

readable, without wrap-around, at a terminal; A. Paul's old output file, OUTPUT, is unchanged and is still available for output to a line printer.

URMEL

Two versions of T. Weiland's (Desy Laboratory, Germany) new URMEL (model analysis of rf cavities) are on CRAY. This latest URMEL incorporates a new eigenvalue-finding routine that calculates all the specified frequencies at once and is much faster. On the CRAY, the single-precision version of the code, URMELF, calculates 13 frequencies in 17 s compared to ∿2.5 min for 2 frequencies from Weiland's earlier version. The double-precision version, URMELFD, takes 5 min to compute the same 13 frequencies. Because the code prints out the relative error of each frequency found, URMELF should be used for general computation; URMELFD should only be used in those cases where better accuracy is desired for the higher modes.

TBCI

All the updates that T. Weiland has forwarded have been incorporated into Weiland's existing TBCI (time domain analysis of beam-cavity interaction) code on the CRAY. In addition, some time was expended in trying to optimize the subroutines that call the plotting routines in order to cut down the running time needed to produce a movie. However, these changes only produced a minimal decrease in running time. It now seems that the DISPLAY plot routines will have to be replaced by much faster 4020 plot routines if there is to be a significant decrease in CPU time.

M3

T. Weiland sent M3 the first part of a code he is developing to do three-dimensional rf cavity analysis. M3 is the input section that generates a three-dimensional mesh and material distribution, and produces three-dimensional plots. We have M3 somewhat running on the CRAY, but Weiland admits there are a number of errors that he is correcting and will be forwarding as a new tape.

POISSON Group Codes

AT-6 has been designated to coordinate the POISSON group codes and to write a new user's guide. During the period, we have established guidelines

to expedite this project. The VAX POISSON group codes, which are R. Holsinger's, (Lab consultant) latest version, have been transferred to the CRAY computer, and these will be the standard versions that will be maintained and updated on the CRAY. However, we have tagged "CRAY" to all instructions added to make the codes operable on the CRAY and commented all constructions that are unique to VAX and/or 7600 by CVAX and C7600, respectively. This makes the codes portable to any of the above machines; the only thing a transferee will have to do is to comment out all "CRAY" instructions and activate the instructions for the particular machine on which the codes will be used. The only changes we are making in these codes at this time are to correct any errors found, such as two errors in LATTICE and one error in SUPERFISH (found by G. Boicourt) and three errors in FORCE (found by M. Menzel). As of now, we have transferred, and have running, the codes for AUTOMESH, LATTICE, POISSON LIBRARY, POISSON, SUPERFISH, and TEKPLOT. These codes have been checked out on all three machines and have produced identical results.

RF STRUCTURES

Cold Models. An 80% scale cold model of the ATS DTL, now under final design, has been constructed and turned over to the structures tuning laboratory. Tests have confirmed the basic design of the DTL to be constructed for ATS. The cold model will be used for studies in voltage ramping techniques.

A 2.5-m-long 600-MHz RFQ cold model has been designed and is now in process of manufacture. This electrically long RFQ model will allow investigation of field stabilization techniques, which would be of advantage in the design of very long RFQs, as well as to help answer other questions concerning RFQ tuning and design.

RFQ Modeling Code. An RFQ modeling code developed by R. M. Hutcheon of Chalk River has been implemented on AT-Division computers. This code is based on a distributed parameter network theory developed at Chalk River by Hutcheon and allows relatively convenient prediction of effects to be expected from modification of such parameters as VCR design, end-tuner variations, and vane modifications. It should prove a valuable adjunct to the RFQ cold-model work.

REFERENCE

1. W. P. Lysenko, "An RFQ Simulation Code," 1984 Linear Accelerator Conf., Darmstadt, Federal Republic of Germany, May 7-11, 1984, Los Alamos National Laboratory document LA-UR-84-1343.

PAPERS PUBLISHED BY ACCELERATOR TECHNOLOGY DIVISION PERSONNEL
(October 1983--March 1984)

Paul Allison and Joseph Sherman, "Operating Experience with a 100-keV, 100-mA H^- Injector," Third Int. Symp. on the Production and Neutralization of Negative Ions and Beams, Brookhaven National Laboratory, Upton, New York, November 14-18, 1983, AIP Conf. Proc. No. 111, American Institute of Physics, New York, 511 (1984).

D. D. Armstrong, W. D. Cornelius, F. O. Purser, R. A. Jameson, and T. P. Wangler, "RFQ Development at Los Alamos," Proc. 1984 Int. Symp. on Heavy-Ion Accelerators and Their Applications to Inertial Fusion, Institute for Nuclear Study January 23-27, 1984, University of Tokyo, Japan, 374 (1983).

G. P. Boicourt, "Radial Particle Distributions in PARMILA Simulation Beams," Particle Accelerators Journal, Los Alamos National Laboratory report LA-10063-MS (March 1984). Also Accelerator Theory Note (AT-6).

C. A. Brau, Compiler, "Los Alamos Free Electron Laser Amplifier Experiment," Los Alamos National Laboratory report LA-UR-84-853 (April 1984).

R. A. Jameson, "Ion Source and Ion Accelerator Development at Los Alamos," Proc. Int. Ion Engineering Congress--ISIAT'83 & IPAT'83, September 12-16, 1983, Kyoto Int. Conf. Hall, Sakyo-ku, Kyoto, Japan, 605 (1983).

R. A. Jameson, "New Linear Accelerators," Institute for Nuclear Study (INS) at INS-Kikuchi Winter School, January 29-February 2, 1984, at Jinzai-Kaihatsu Center, 1400 Shin'ya, Fujiyoshida, Yamanashi 403, Japan, Los Alamos National Laboratory document LA-UR-84-25.

Andrew J. Jason and George P. Lawrence, "LIRIC: A Preliminary Design Study of the Próton Driver for a New ORNL Neutron Source," Documentation of a design study conducted for Oak Ridge National Laboratory by the Los Alamos Accelerator Technology Division, Los Alamos National Laboratory document LA-UR-83-2807 (February 1984).

E. L. Kemp, "The Status of the FMIT Accelerator," Fusion Engineering Symposium, Philadelphia, Pennsylvania, December 5-9, 1983, Los Alamos National Laboratory document LA-UR-83-3390.

David Neuffer, "A Lattice for a 'Low-Field' Superconducting Super Collider," Proc. of Ann Arbor Workshop on Accelerator Physics Issues for a Superconducting Super Collider, Ann Arbor, Michigan, December 11-17, 1983, Los Alamos National Laboratory document LA-UR-84-191.

D. Neuffer, "Principles and Applications of Muon Cooling," Particle Accelerators, 14, 75-90 (1983).

H. Vernon Smith, Jr., Paul Allison, and Joseph D. Sherman, "A Scaled, Circular-Emitter Penning SPS for Intense H^- Beams," Third Int. Symp. on the Production and Neutralization of Negative Ions and Beams, Brookhaven National Laboratory, Upton, New York, November 14-18, 1983, AIP Conf. Proc. No. 111, American Institute of Physics, New York, 458 (1984).

T. P. Wangler, "Some Design Constraints for an RF-Linac/Storage-Ring Driver," Proc. 1984 Int. Symp. on Heavy-Ion Accelerators and Their Applications to Inertial Fusion, Institute for Nuclear Study January 23-27, 1984, University of Tokyo, Japan, 222 (1984).

R. W. Warren, B. E. Newnam, W. E. Stein, J. G. Winston, R. L. Sheffield, M. T. Lynch, J. C. Goldstein, M. C. Whitehead, O. R. Norris, G. Leudemann, T. O. Gibson, and C. M. Humphry, "First operation of the Los Alamos Free-Electron Laser Oscillator," Sixth Int. Conf. on Lasers & Applications, LASERS '83, San Francisco, California, December 12-16, 1983. Sponsored by Society for Optical and Quantum Electronics. Los Alamos National Laboratory document LA-UR-84-202.

S. L. Wipf, "Dipole Aperture and Superconductor Requirements," Proc. Ann Arbor Workshop on Accelerator Physics Issues for a Superconducting Super Collider, Ann Arbor, Michigan, December 11-17, 1983, Los Alamos National Laboratory document LA-UR-84-96.

Accelerator Theory Notes (AT-6)

J. L. Warren, "Determination of Magnet Misalignments from Measurement of Closed Orbit Distortion," AT-6:ATN-83-13 (March 1983). (PSR TECHNICAL NOTE 111)

Tai-Sen F. Wang, "Bunch Extractions in the 503.125 MHz RF System," AT-6:ATN-83-14 (April 1983). (PSR Technical Note 115)

M. H. Foss, "AGS Space Charge Limit," AT-6:ATN-83-15 (July 1983).

W. Lysenko, "Using the CD/2000 CAD/CAM System for Software Documentation," AT-6:ATN-83-16 (July 1983).

E. Forest and J. L. Warren, "Application of Symplectic Conditions to Second Order Transport Theory," AT-6:ATN-83-17 (May 1984).

P. J. Channell, "Initial Value and Eigenvalue Problems for Field Equations Using Symplectic Integration Algorithms," AT-6:ATN-83-18 (August 1983).

P. J. Channell, "Numerical Generation of KV Distributions," AT-6:ATN-83-19 (August 1983).

P.J. Channell, "The Ponderomotive Force Due to a Doubly Periodic Force," AT-6:ATN-83-20 (August 1983).

P. J. Channell, "Drift Waves in an H^- Source," AT-6:ATN-83-21 (August 1983).

W. Lysenko, "RFQTEP: A Fast 3-D RFQ Simulation Code," AT-6:ATN-83-22 (August 1983).

G. P. Boicourt, "On Errors in Using an Axial Power Series Expansion for the Vector Potential," AT-6:ATN-83-23 (August 1983).

E. Forest, "Computation of Chromaticities Using Lie Algebraic Polynomials," AT-6:ATN-83-24 (August 1983).

W. Lysenko, "Voltage Droop Simulations for the ATS RFQ," AT-6:ATN-83-25 (August 1983).

W. Lysenko and J. Warren, "Report on Frontiers in Supercomputing Conference," AT-6:ATN-83-26 (September 1983).

Tai-Sen Wang, "On Beam Injection in the Short Bunch Operating Mode," AT-6:ATN-83-27 (October 1983).

D. Neuffer, "Some Thoughts on Luminosity, Tune Shift, Lattice, and Instability Constraints on a Super Collider," AT-6:ATN-83-28 (December 1983).

W. Lysenko, "The RFQ Simulation Code Library RFQLIB and Associated Codes," AT-6:ATN-84-1 (January 1984).

W. Lysenko, "RFQ Acceptance Computations," AT-6:ATN-84-2 (January 1984).

W. Lysenko, "A New Beam Dynamics Code and How to Write Physics Programs," AT-6:ATN-84-3, LA-UR-84-1402 (March 1984).

David Neuffer, "Beam-Beam Interaction and the SSC," AT-6:ATN-84-4 (March 1984).

Technical Memorandum AT-6

G. P. Boicourt, POWER LOSS AND FREQUENCY PERTURBATION ESTIMATES FOR THE ATS-DTL 2nd DESIGN, AT-6:84-17 (March 9, 1984.)

GROUP AT-1 TECHNICAL MEMO INDEX

Comments on the Dipole Induced Torque Effect in the RFQ	K. R. Crandall, T. P. Wangler	AT-1:83-316	10/14/83
Comparison of Illinois Coax Structure with Side-Coupled Structure	L. Young	AT-1:83-318	10/17/83
Magnetic Insulation for RFQ Linacs--An Idea with Significant Potential	T. P. Wangler	AT-1:83-336	11/8/83
Lumped-Circuit Model of 4-Vane RFQ Resonator	T. P. Wangler	AT-1:83-348	11/15/83
Drift-Tube Linac Post Couplers and the Poynting Vector--An Elementary Physics Picture	T. P. Wangler	AT-1:83-352	11/18/83
RFQ Current Limit Dependence on Peak Surface Electric Field	T. P. Wangler	AT-1:83-378	12/13/83
Q Measurement Technique	L. Young	AT-1:83-382	12/16/83
Frequency Response of RTM Phase and Amplitude Feedback Controllers	L. Young	AT-1:83-386	12/16/83
H^- TDA Design Including Matching	K. R. Crandall, R. S. Mills	AT-1:83-385	12/16/83
PSR 503-MHz Ferrite Thermal Analysis	L. Hansborough	AT-1:84-2	1/03/84
Brazing Process for PSR Buncher	P. L. Roybal	AT-1:84-8	1/11/84
PARMTEQ Runs for AT-2 RFQ2 Measured Fields	K. Crandall, R. Mills	AT-1:84-9	1/11/84
Alternative Longitudinal Match for H^- TDA Design	K. R. Crandall, R. S. Mills	AT-1:84-23WH	1/20/84
Alternate Routes to 50 MeV	R. S. Mills	AT-1:84-47WH (Revised)	2/03/84
Intentional and Unintentional Beam Deflection	R. H. Stokes, K. R. Crandall, R. S. Mills	AT-1:84-58	2/13/84
Survey of Drift-Tube Linacs with Post Couplers	J. H. Billen	AT-1:84-74	2/27/84

The Effect of Cutting Speed and Tool Type on the Q of an Accelerating Cavity	L. Young	AT-1:84-82	3/01/84
New Drift Tube Tables for AT2-DTL	R. S. Mills K. R. Crandall	AT-1:84-86	3/01/84
Field Tilts in Drift-Tube Linacs	J. H. Billen	AT-1:84-100	3/09/84

GROUP AT-3 TECHNICAL MEMO INDEX
TECHNICAL NOTES

Title	Authors	Document No.	Date
An Electrical Investigation of the Explosively Hydroformed Beam Positior Sensor	G. Paffenroth	PSR T.N. 121	10/83
Some PSR I&C Signal Connections	A. Conley	PSR T.N. 122	11/83
Switchyard Kicker Pulse Forming Network Charging System and D.C. Power Supply Ratings	E. F. Higgins	PSR T.N. 123	6/84
Phase Matching Cable Pairs for the PSR Beam Position Monitor System	F. D. Wells P. C. Dowden	PSR T.N. 124	3/84
Proton Storage Ring Instrumentation and Control System Signal Connection Manual	P. Clout	PSR T.N. 125	3/84

U.S. GOVERNMENT PRINTING OFFICE 1985—576-034/20002